NASA/TP-1998-208421

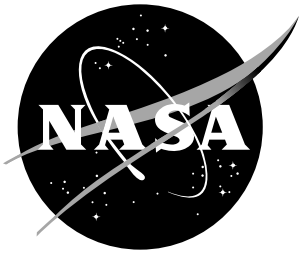

Evaluation of the Transient Liquid Phase (TLP) Bonding Process for Ti_3Al-Based Honeycomb Core Sandwich Structure

R. Keith Bird and Eric K. Hoffman
Langley Research Center, Hampton, Virginia

June 1998

The NASA STI Program Office ... in Profile

Since its founding, NASA has been dedicated to the advancement of aeronautics and space science. The NASA Scientific and Technical Information (STI) Program Office plays a key part in helping NASA maintain this important role.

The NASA STI Program Office is operated by Langley Research Center, the lead center for NASA's scientific and technical information. The NASA STI Program Office provides access to the NASA STI Database, the largest collection of aeronautical and space science STI in the world. The Program Office is also NASA's institutional mechanism for disseminating the results of its research and development activities. These results are published by NASA in the NASA STI Report Series, which includes the following report types:

- TECHNICAL PUBLICATION. Reports of completed research or a major significant phase of research that present the results of NASA programs and include extensive data or theoretical analysis. Includes compilations of significant scientific and technical data and information deemed to be of continuing reference value. NASA counter-part of peer reviewed formal professional papers, but having less stringent limitations on manuscript length and extent of graphic presentations.

- TECHNICAL MEMORANDUM. Scientific and technical findings that are preliminary or of specialized interest, e.g., quick release reports, working papers, and bibliographies that contain minimal annotation. Does not contain extensive analysis.

- CONTRACTOR REPORT. Scientific and technical findings by NASA-sponsored contractors and grantees.

- CONFERENCE PUBLICATION. Collected papers from scientific and technical conferences, symposia, seminars, or other meetings sponsored or co-sponsored by NASA.

- SPECIAL PUBLICATION. Scientific, technical, or historical information from NASA programs, projects, and missions, often concerned with subjects having substantial public interest.

- TECHNICAL TRANSLATION. English-language translations of foreign scientific and technical material pertinent to NASA's mission.

Specialized services that help round out the STI Program Office's diverse offerings include creating custom thesauri, building customized databases, organizing and publishing research results ... even providing videos.

For more information about the NASA STI Program Office, see the following:

- Access the NASA STI Program Home Page at ***http://www.sti.nasa.gov***

- E-mail your question via the Internet to help@sti.nasa.gov

- Fax your question to the NASA Access Help Desk at (301) 621-0134

- Phone the NASA Access Help Desk at (301) 621-0390

- Write to:
  NASA Access Help Desk
  NASA Center for AeroSpace Information
  7121 Standard Drive
  Hanover, MD 21076-1320

NASA/TP-1998-208421

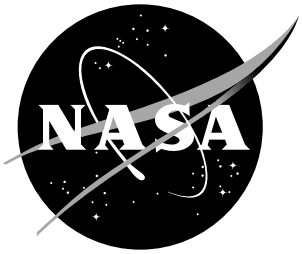

Evaluation of the Transient Liquid Phase (TLP) Bonding Process for Ti_3Al-Based Honeycomb Core Sandwich Structure

R. Keith Bird and Eric K. Hoffman
Langley Research Center, Hampton, Virginia

National Aeronautics and
Space Administration

Langley Research Center
Hampton, Virginia 23681-2199

June 1998

ACKNOWLEDGMENT

The authors would like to express their appreciation to Stephanie Chiras for her contribution to this research project. Ms. Chiras was a summer student from Harvard University, and she was responsible for the testing and data analysis for a large number of the edgewise compression tests. Ms. Chiras conducted an extensive amount of testing over a short period of time to help complete this research project.

Summary

The suitability of using transient liquid phase (TLP) bonding to fabricate honeycomb core sandwich panels with Ti-14Al-21Nb (wt%) titanium aluminide (Ti_3Al) face sheets for high-temperature hypersonic vehicle applications was evaluated. The TLP bonding process involves using a foil filler metal between the mating titanium honeycomb sandwich components that produces a eutectic liquid phase to assist in the diffusion bonding. Three titanium alloy honeycomb cores (Ti-3Al-2.5V, Ti-6Al-4V, and Ti-15V-3Cr-3Sn-3Al) and one Ti_3Al alloy honeycomb core (Ti-14Al-21Nb) were investigated. Structural properties of the honeycomb core sandwich panels were determined using edgewise compression (EWC) tests and the strength of the joint between the face sheet and honeycomb was evaluated using flatwise tension (FWT) tests. In addition, tensile tests were conducted on the Ti-14Al-21Nb face sheet material to determine the effects of processing on the face sheet properties. FWT, EWC, and tensile tests were conducted at temperatures ranging from room temperature to 1500°F.

EWC tests indicated that the honeycomb cores and diffusion bonded joints were able to stabilize the face sheets up to and beyond the face sheet compressive yield strength for all temperatures investigated. The Ti-15V-3Cr-3Sn-3Al specimens produced the highest FWT strengths over the temperature range from room temperature to 1000°F. At temperatures above 1000°F, the Ti-14Al-21Nb specimens produced the highest FWT strengths.

Tensile tests of the Ti-14Al-21Nb face sheet material indicated that the processing conditions used to fabricate the three titanium alloy honeycomb core sandwich panels caused a decrease in face sheet strength, an increase in modulus, and a minor decrease in ductility compared to unprocessed α/β solution treated Ti-14Al-21Nb sheet material. The processing conditions used to fabricate the sandwich panel with Ti-14Al-21Nb honeycomb core resulted in a significant loss of face sheet ductility and tensile strength at room temperature.

Microstructural examination showed that the side of the face sheets to which the filler metals had been applied was transformed from equiaxed α_2 grains to coarse plates of α_2 with intergranular β. Fractographic examination of the tensile specimens showed that this transformed region was dominated by brittle fracture.

The results from this study indicate that TLP bonding has good potential for fabricating lightweight honeycomb core sandwich structure with titanium aluminide face sheets and titanium aluminide or conventional titanium alloy honeycomb core suitable for high-temperature hypersonic vehicle applications.

Symbols and Abbreviations

α	hexagonal close-packed titanium
α_2	ordered Ti_3Al intermetallic
β	body-centered cubic titanium
e_p	plastic tensile strain to failure
E	tensile modulus of elasticity
EDS	energy dispersive x-ray spectroscopy
EWC	edgewise compression
FWT	flatwise tension
SEM	scanning electron microscopy
Ti-14-21	alloy Ti-14Al-21Nb (wt%)
Ti-15-3	alloy Ti-15V-3Cr-3Sn-3Al (wt%)
Ti-3-2.5	alloy Ti-3Al-2.5V (wt%)
Ti-6-4	alloy Ti-6Al-4V (wt%)

TLP	transient liquid phase
UTS	ultimate tensile strength
WDS	wavelength dispersive x-ray spectroscopy
YS	0.2%-offset tensile yield strength

Introduction

The successful deployment of high-speed aircraft having a sustained hypersonic cruise capability is highly dependent upon the development of lightweight, high-temperature structures (ref. 1–3). The structural concepts for this type of vehicle call for high-stiffness, thin-gage product forms that can be fabricated into efficient, load-bearing components. Titanium-based materials are considered prime candidates for large-scale structural use in the airframe because of their low density and good properties at temperatures up to 800°F. In sheet form they could provide the basis for efficient, lightweight honeycomb core sandwich structure. To achieve the performance goals for a hypersonic vehicle airframe, however, it is critical that the temperature capability of the titanium honeycomb core sandwich structure be extended to even higher operating temperatures so that the need for structural cooling can be minimized. Over the last few years, a new class of material based on the α_2 titanium aluminide intermetallic (Ti_3Al) composition has emerged. Ti_3Al-based alloys have improved high-temperature properties and lower densities compared to those for conventional titanium alloys (ref. 1,4). Structures fabricated from Ti_3Al have the potential for high strength- and stiffness-to-weight ratios at the temperatures of interest for hypersonic flight. The primary drawback with utilizing Ti_3Al is the inherently low room temperature ductility and toughness (ref. 1,5,6), which can have serious implications for the integrity of such a structure. Extensive research (ref. 3,5,6), however, has resulted in an increase in the room temperature ductility of the Ti_3Al to acceptable levels through niobium alloying additions. One such alloy of particular interest is Ti-14Al-21Nb (Ti-14-21).

The development of processing and joining techniques for the incorporation of Ti_3Al into honeycomb core sandwich structure is critical to the construction of hypersonic aircraft components (ref. 1). The joining techniques must produce joints with adequate strength at service temperatures without significantly degrading the properties of the component materials. A state-of-the-art commercial joining process that was developed for fabricating titanium alloy honeycomb core sandwich structure is the RohrBond[1] process. RohrBond is a diffusion-assisted bonding process that utilizes a eutectic liquid phase to assist in the diffusion bonding of the mating titanium honeycomb sandwich components. RohrBond, known generically as transient liquid phase (TLP) bonding, is described in detail in ref. 7–12. This process has several advantages over conventional diffusion bonding and brazing and is a candidate for fabricating Ti_3Al-based honeycomb core sandwich structure.

This study was conducted to evaluate the suitability of the TLP bonding process for the fabrication of honeycomb core sandwich panels with Ti-14-21 components. Sandwich panels were fabricated by Rohr, Inc., using Ti-14-21 face sheets and various titanium alloy honeycomb core materials. Specimens cut from honeycomb core sandwich panels were tested in edgewise compression (EWC) to measure the structural behavior and in flatwise tension (FWT) to measure the strength of the diffusion bonded joint between the face sheet and honeycomb core. In addition, tensile tests were conducted on the Ti-14-21 face sheet material to determine the effect of processing on the face sheet properties. FWT, EWC, and tensile tests were conducted at temperatures ranging from room temperature to 1500°F. Fractography and metallurgical analysis were used to correlate properties and microstructure.

[1]RohrBond is a registered trademark of Rohr, Inc.

TLP Bonding

In the TLP bonding process, an intermediate foil filler metal, usually based on copper, is placed between the titanium components to be joined. When heated above the titanium/filler metal eutectic temperature for a sufficient period of time, the titanium and filler metal interdiffuse to form a eutectic composition. As a result, a eutectic liquid forms and fills the gaps at the joint interface. This liquid phase enhances diffusivity and ensures intimate contact at the joint interface without the high bonding pressures and close surface tolerances required by conventional diffusion bonding. The components are held at this temperature during which time the liquid solute elements diffuse into the titanium components. With continuing solute diffusion, the melt composition becomes titanium-enriched resulting in an increase in the melting temperature and eventual isothermal solidification. Additional time at temperature permits solid-state diffusion to dilute the solute concentration even further, resulting in improved mechanical properties of the joint. After this bonding period, the components are allowed to slow cool in the vacuum furnace.

Experimental Procedures

Materials

Four honeycomb core sandwich panels were fabricated by Rohr, Inc., Chula Vista, California. Each panel was 21 inches by 30 inches and consisted of two 0.020-inch-thick Ti-14-21 face sheets TLP bonded to a 0.6-inch-thick honeycomb core. A different honeycomb core alloy was utilized for each sandwich panel: $\alpha + \beta$ titanium alloys Ti-3Al-2.5V (Ti-3-2.5) and Ti-6Al-4V (Ti-6-4); β titanium alloy Ti-15V-3Cr-3Sn-3Al (Ti-15-3); and Ti_3Al alloy Ti-14-21. The $\alpha + \beta$ and β cores were formed into 0.25-inch corrugated square cells from 0.002-inch-thick foil. Due to the limited ductility of the Ti-14-21 alloy, the alloy could not be rolled to as thin a gage nor fabricated into as small a cell size as that for $\alpha + \beta$ and β titanium alloys. Therefore, the Ti-14-21 core was formed into 0.375-inch corrugated square cells from 0.004-inch-thick foil. Figure 1 shows a picture of the Ti-14-21 honeycomb core sandwich panel.

Rohr used two proprietary TLP bonding processes to fabricate the sandwich panels. The first process, designated LID, was used to fabricate the Ti-3-2.5, Ti-6-4, and Ti-15-3 honeycomb core sandwich panels. The LID filler metal used to join the face sheets to the honeycomb core was a Cu/Ni alloy. The second TLP process, designated Pro-4, was used to fabricate the Ti-14-21 honeycomb core sandwich panel. The Pro-4 process used a different filler metal composition (Cu/Sn alloy), and required a higher bonding temperature and a longer bonding time than the LID process. Table 1 summarizes the physical description of each panel.

Metallurgical Analysis

Metallurgical specimens were sectioned from the honeycomb core sandwich panels using a diamond-wheel saw and were mounted in an epoxy medium. Following polishing, the specimen surface was etched using Kroll's reagent. The specimens were examined using optical microscopy and scanning electron microscopy (SEM) to characterize the microstructure. Energy and wavelength dispersive x-ray spectroscopy (EDS and WDS) were used to determine the face sheet/core joint interface elemental concentration profiles. In addition, the fracture surface morphology of the face sheet tensile specimens was characterized using SEM analysis.

Test Specimens

Flatwise tension and edgewise compression tests were used to evaluate the honeycomb core sandwich panels. Each panel was sectioned into 24 FWT and 24 EWC test specimens using wire electrical discharge machining. The nominal dimensions of the FWT specimens were 2 inches long by 2 inches wide while those of the EWC specimens were 6.5 inches long by 2.5 inches wide. The EWC specimens were machined such that the honeycomb core foil ribbon was oriented parallel to the specimen length.

Tensile tests were used to evaluate the effect of LID and Pro-4 processing on the mechanical properties of the face sheets. The honeycomb core was cut from untested EWC specimens using a band saw. The remaining honeycomb core "stubble" was ground from the face sheets with a SiC grinding wheel to produce a smooth test specimen. The ground face sheets were then machined into subsize tensile specimens, as per ASTM specification E8-91 (ref. 13). The specimens measured 4.0 inches long by 0.375 inch wide with a reduced test section measuring 1.25 inches long by 0.25 inch wide. For comparative purposes, tensile specimens were also machined from 0.020-inch thick Ti-14-21 sheet in the unprocessed α/β solution treated condition to obtain a baseline set of tensile properties for the face sheet material prior to TLP processing.

Mechanical Testing

Face sheet tensile tests

The TLP-processed face sheet tensile specimens were tested at temperatures ranging from room temperature to 1500°F depending upon the projected maximum service temperature for each honeycomb core sandwich panel. The α/β solution treated sheet specimens were tested at room temperature and 1200°F. Tensile properties determined included ultimate tensile strength (UTS), yield strength (YS), modulus (E), and plastic strain to failure (e_p). All tensile tests were conducted with a servo-hydraulic test machine using hydraulic grips. For the elevated temperature tests, the specimens and grips were heated with a resistance-heated, three-zone, split tube furnace. Specimen temperature was measured with thermocouples attached to the center of the specimen gage section and to the top and bottom grips. The heat-up time was approximately one hour, and the specimens were allowed to soak at the test temperature for five minutes prior to loading. Temperature uniformity over the specimen gage length was within ±3°F of the desired test temperature for the duration of the test. An actuator displacement rate of 0.010 in/min was used until a total strain of 2% was attained, at which time the rate was increased to 0.050 in/min.

Room temperature strain was measured with extensometers attached to the front and back faces of the specimen. Due to space constraints within the furnace, only a single water-cooled, high-temperature extensometer was used to measure elevated temperature strain. The high-temperature extensometer used quartz extension rods which passed through the furnace wall and attached to the face of the specimen. All extensometers had a one-inch gage length.

Flatwise tension tests

Flatwise tension tests were used to measure the core-to-face sheet joint strength. The tests consisted of subjecting a sandwich specimen to tensile loads normal to the plane of the face sheets; these loads are transmitted to the specimen through thick loading blocks attached to the face sheets. The FWT tests were conducted in accordance with ASTM specification C297 (ref. 14). To accommodate the elevated temperature tests, the FWT specimens were vacuum brazed to one-inch thick Ti-6-4 loading blocks using Cu foil filler metal at 1750°F for 30 minutes. The FWT specimens were loaded in a screw-driven test machine via threaded holes in the back of the loading blocks. Figure 2 shows a FWT specimen inside the test apparatus. FWT tests for the respective honeycomb core sandwich specimens were conducted at temperatures ranging from room temperature to 1500°F depending on the projected maximum service temperature for each core material. The elevated temperature specimens were heated with a resistance-heated, three-zone, split tube furnace. Thermocouples were resistance spot welded to the front and back faces of each loading block to monitor specimen temperature. Each specimen was held at the desired test temperature (±10°F) for 10 minutes prior to being loaded to failure at a rate of 250 lbs/min. The FWT strength was calculated by dividing the maximum load by the face sheet area.

Edgewise compression tests

The edgewise compression test is designed to determine the compressive properties of the specimens when loaded in a direction parallel to the plane of the face sheets. EWC strength is a measure of the ability of the core and the joints to stabilize the face sheets in compression. The EWC tests were conducted in accordance with ASTM specification C364 (ref. 15). The specimens were tested in a specially designed compression cage EWC test fixture using a screw-driven test machine. Figure 3 shows an EWC specimen mounted in the test apparatus. The specimens were tested at temperatures ranging from room temperature to 1500°F depending on the projected maximum service temperature for each honeycomb core material. Elevated temperature tests were conducted in a resistance-heated, three-zone, split tube furnace mounted to the test stand. Six thermocouples were distributed along the length of the front and back face sheets to monitor specimen temperature. Each specimen was held at the desired test temperature (±10°F) for 10 minutes prior to being loaded to failure at a rate of 2000 lbs/min. Strain for both the front and back face sheets was measured with foil strain gages at room temperature and water-cooled extensometers at elevated temperature. EWC strength was calculated by dividing the failure load by the cross-sectional area of both face sheets.

Results and Discussion

Metallurgical Analysis

LID-processed panels

Figure 4 shows representative optical photomicrographs of LID-processed honeycomb core sandwich panel joints fabricated with Ti-3-2.5, Ti-15-3, and Ti-6-4 honeycomb cores. Large fillets formed at the face sheet/core nodes as a result of capillary attraction of the molten filler metal. No deleterious erosion of the foil gage honeycomb core due to core/filler metal interaction was observed. The majority of the joints that were examined in these panels were well-diffused and had a fine multiphase structure. A small number of the joints that were examined had regions where the molten filler metal pooled at the core/face sheet interface and formed undiffused regions which may result in localized regions of lower joint strength. A small undiffused region within the joint can be seen in the photomicrograph of the Ti-6-4 honeycomb core panel shown in figure 4.

Figure 5 shows the microstructure of the face sheet remote from the joint in the Ti-3-2.5 honeycomb core sandwich panel. The microstructure of the Ti-14-21 face sheet bulk material consisted of equiaxed α_2 grains with β at the grain boundaries. The surface of the face sheet to which the LID filler metal had been applied was characterized by a 50-μm-thick transformed region consisting of coarse α_2 laths separated by intergranular β. This transformed region resulted from diffusion of the β-stabilizing Cu and Ni constituents of the filler metal into the face sheet. Cu- and Ni-enrichment of the β phase contained within the transformed region was verified by EDS x-ray mapping. (See fig. 6.)

All three of the LID-processed panels exhibited similar face sheet and joint microstructures. Only the microstructures of the honeycomb core remote from the joint differed. Figure 7 shows the honeycomb core microstructures remote from the joint for LID-processed Ti-3-2.5, Ti-6-4, and Ti-15-3 honeycomb core sandwich panels. The apparent thickness of the cell walls for the three honeycomb core samples is a function of the angle at which the metallurgical sections were taken. All three of the honeycomb core cell walls were 0.002 inch thick. The Ti-3-2.5 and Ti-6-4 honeycomb core microstructures consisted of coarse α plates separated by intergranular β. The microstructure of the Ti-15-3 honeycomb core consisted of large β grains extending through the entire thickness of the foil gage cell wall, with fine plates of α decorating the grain boundaries.

Figure 8 shows an SEM photomicrograph of a joint from a LID-processed Ti-6-4 honeycomb core sandwich panel. Also shown is a WDS ele-

mental concentration profile of the LID filler metal constituents Cu and Ni across the joint interface. The original interface was assumed to correspond to the edge of the face sheet. The scans began 100 μm into the face sheet and extended 200 μm into the honeycomb core with a scan step distance of 10 μm.

The plot shows that the maximum Cu and Ni concentrations were shifted from the original joint interface approximately 50 μm into the honeycomb core. The concentrations tended to vary sharply within the joint. This behavior occurred because of differences in composition of individual phases contained within the fine multiphase joint microstructure. The relative concentrations and depths of diffusion of Cu and Ni were much greater in the Ti-6-4 honeycomb core than in the Ti-14-21 face sheet. At the LID processing temperature, the Ti-6-4 honeycomb core consisted of all β phase whereas the Ti-14-21 face sheet contained ordered α_2 phase. The greater concentrations of Cu and Ni in the honeycomb core were attributed to Cu and Ni diffusing more rapidly into β-Ti than into ordered α_2 and capillary flow of the molten LID filler metal along the honeycomb core cell walls.

Pro-4-processed panel

Figure 9 shows an optical photomicrograph of a joint from the Pro-4-processed Ti-14-21 honeycomb core sandwich panel. The large fillets at the face sheet/core nodes and the well-diffused, multi-phase joints were similar in appearance to the joints in the LID-processed panels. In addition, no deleterious erosion of the honeycomb core was observed. Figure 10 shows the Ti-14-21 face sheet microstructure remote from the joint. The microstructure of the Ti-14-21 face sheet bulk material was characterized by equiaxed α_2 grains with β at the grain boundaries. This microstructure was similar in appearance to that of the LID-processed Ti-14-21 face sheet bulk material (fig. 5), except that the β phase in the grain boundaries had coarsened and become more continuous. The surface of the face sheet to which the Pro-4 filler metal had been applied exhibited a transformed region which consisted of finer α_2 laths with higher aspect ratios than those in the LID-processed Ti-14-21 face sheets. In addition, the depth of this transformed region extended to a greater depth (90 μm) due to the higher temperature and longer time associated with the Pro-4 processing cycle.

Figure 11 shows the Pro-4-processed Ti-14-21 honeycomb core microstructure remote from the joint. The outer edges of the core cell walls consisted of α_2 laths and intergranular β while the interior consisted of equiaxed α_2 with β at the grain boundary triple points. This transformed microstructure was caused by capillary flow of the molten filler metal along the surface of the honeycomb core cell walls and its subsequent diffusion into the outer edges of the honeycomb core.

Figure 12 shows an SEM photomicrograph of a Pro-4-processed Ti-14-21 honeycomb core sandwich panel joint. Also shown is a WDS chemical concentration profile of the Pro-4 filler metal constituents Cu and Sn across the joint interface. The original interface was assumed to correspond to the edge of the face sheet. The scans began 200 μm into the face sheet and extended 300 μm into the honeycomb core with a scan step distance of 10 μm.

The plots show that the maximum Cu and Sn concentrations occurred in the honeycomb core approximately 50 μm from the joint interface. The concentrations tended to vary sharply within the fine multiphase joint microstructure. The depth of Cu and Sn diffusion in the Ti-14-21 honeycomb core was greater than in the Ti-14-21 face sheets. This was attributed to capillary flow of the molten Pro-4 filler metal along the honeycomb core cell walls and the slower bulk diffusion into the face sheets than surface diffusivity into the honeycomb core. Within the joint, a greater concentration of Cu was detected than Sn. This concentration difference was attributed to differences in the starting composition of the two filler metals and to differences in diffusivity of the two elements.

In comparing the concentration profiles for the

Pro-4- and LID-processed joints, the Pro-4 process resulted in greater concentrations and greater depth of diffusion of Cu in the face sheet and honeycomb core. The difference in the depth of diffusion was attributed to the higher temperature and longer time associated with the Pro-4 processing cycle while the concentration difference was attributed to the differences in starting Cu composition between the LID and Pro-4 filler metals.

Face Sheet Tensile Tests

The Ti-14-21 face sheet tensile data for the LID- and Pro-4-processed honeycomb core sandwich panels are shown in figures 13–16. A complete tabulation of the tensile test data is shown in Appendix A. Figure 13 shows the average room and elevated temperature UTS and YS of the Ti-14-21 face sheet specimens from the three LID-processed panels. Also shown for comparison are the average UTS and YS at room temperature and 1200°F for unprocessed Ti-14-21 sheet in the α/β solution treated condition. The room temperature UTS and YS of unprocessed Ti-14-21 sheet were 91 ksi and 82 ksi, respectively. As compared to the unprocessed sheet, the LID-processed face sheets exhibited lower UTS ranging from 78 ksi to 81 ksi and lower YS ranging from 64 ksi to 70 ksi. At 1200°F, the unprocessed sheet had UTS of 51 ksi and YS of 40 ksi. The LID-processed face sheets exhibited lower YS ranging from 28 ksi to 33 ksi, but the UTS (43–53 ksi) was approximately the same as that for the unprocessed sheet. The face sheets from the three panels had similar strength behavior because they all were exposed to the same processing conditions. The UTS of the LID-processed sheets increased slightly from room temperature to 800°F, then decreased sharply with increasing temperature. The YS for the LID-processed face sheets decreased continuously with increasing temperature.

Figure 14 shows the average room and elevated temperature UTS and YS values for the Pro-4-processed Ti-14-21 face sheet specimens. Also shown for reference is the UTS and YS data ranges for the LID-processed Ti-14-21 face sheet specimens from figure 13. The Pro-4-processed specimens were exposed to a higher temperature, a longer time, and a different filler metal composition than the LID-processed specimens. At room temperature and 800°F, the UTS for the Pro-4-processed Ti-14-21 specimens was significantly less than that for the LID-processed specimens. At temperatures of 1000°F and above, the UTS values for the Pro-4- and LID-processed specimens were equivalent. The YS of the Pro-4-processed Ti-14-21 face sheet specimens correlated well with that for the LID-processed specimens at all temperatures tested.

The average room and elevated temperature ductilities, as measured by e_p, for the LID- and Pro-4-processed Ti-14-21 face sheet specimens and the unprocessed Ti-14-21 sheet in the α/β solution treated condition are shown in figure 15. The room temperature ductility of unprocessed Ti-14-21 sheet was 3.0%. After exposure to the LID-processing cycle, the Ti-14-21 still retained most of its room temperature ductility (e_p = 1.8–2.8%); however, Pro-4 processing embrittled the Ti-14-21 (e_p = 0.2%). The face sheet ductility of the LID-processed specimens increased rapidly with temperature up to 800°F. At temperatures of 800°F and higher, the e_p was so high (>12%) that the tests were stopped prior to specimen failure. Although the ductility of the Pro-4-processed specimens gradually increased with temperature, the e_p was still relatively low (3.9%) at 1000°F. Only at 1300°F and 1500°F did any of these specimens attain 12% plastic strain without failure.

Figure 16 shows the average room and elevated temperature E values for the LID- and Pro-4-processed Ti-14-21 face sheet specimens and the unprocessed Ti-14-21 sheet in the α/β solution treated condition. The room temperature E of unprocessed Ti-14-21 was 10.4 Msi. After exposure to the LID-processing cycle, the room temperature E of the Ti-14-21 increased to an average value ranging from 11.6 Msi to 13.4 Msi. Similarly, the room temperature E for the Pro-4-processed specimens increased to 12.7 Msi. All four data curves show that E decreased gradually with temperature to 800°F, then decreased rapidly at the higher temperatures. At 1200°F, the E

for the LID- and Pro-4-processed sheet was approximately the same as that for the unprocessed sheet.

Figure 17 shows the room temperature fracture surface of a LID-processed Ti-14-21 face sheet tensile specimen. The LID-transformed region of the microstructure (see fig. 5) produced a different fracture morphology than did the microstructure remote from the transformed region. In the LID-transformed region, the fracture surface was characterized by intergranular fracture along the coarse α_2 laths with some distinct regions of ductile microvoid coalescence corresponding to the β phase. The remainder of the fracture surface remote from the LID-transformed region exhibited intergranular fracture of the equiaxed α_2 grains. These fracture surface features were typical for all the LID-processed Ti-14-21 face sheet tensile specimens, regardless of the type of honeycomb core to which they were originally bonded.

Figure 18 shows the room temperature fracture surface of a Pro-4-processed Ti-14-21 face sheet tensile specimen. The Pro-4-transformed region of the microstructure (see fig. 10) produced a different fracture morphology than did the microstructure remote from the transformed region. The specimen exhibited brittle fracture along the entire Pro-4-transformed region, which comprised approximately 20% of the face-sheet cross-section. No signs of ductile microvoid coalescence were evident. The high Cu concentrations in the transformed region may have contributed to the brittle fracture morphology observed in this region. The addition of Cu has been previously associated with the formation of brittle compounds such as Ti_2Cu (ref. 16). The fracture surface remote from the transformed region exhibited intergranular fracture of the equiaxed α_2 grains that was similar in appearance to that observed for the LID-processed face sheets.

LID-processing of the Ti-14-21 face sheet material caused a decrease in room temperature UTS and YS, an increase in E, and a minor decrease in e_p in comparison to unprocessed Ti-14-21 sheet tensile properties. The Pro-4-processed face sheets showed the same YS and E trends as did the LID-processed face sheets. However, Pro-4 processing caused a significant reduction in room temperature face sheet ductility and UTS in comparison to the LID-processed face sheet tensile properties. This reduction in room temperture properties is most likely due to the the greater depth of Cu diffusion into the Pro-4-processed face sheets than was observed in the LID-processed face sheets. This embrittlement could potentially be reduced by lowering the processing temperature and time and minimizing the amount of filler metal used to fabricate the panel.

Flatwise Tension Tests

The average room and elevated temperature FWT strengths for the LID- and Pro-4-processed honeycomb core sandwich specimens are shown in figure 19. A complete tabulation of the FWT test data is shown in Appendix B. The plot shows that the LID-processed Ti-15-3 honeycomb core sandwich specimens had the highest FWT strength at temperatures up to 1000°F. At temperatures above 1000°F, the FWT strength of all three types of LID-processed specimens decreased rapidly. Although the Pro-4-processed Ti-14-21 honeycomb core sandwich specimens had the lowest FWT strength at room temperature, they also had the highest FWT strength at temperatures above 1000°F. The FWT strength of the Ti-14-21 specimens did not begin to decrease until the temperature exceeded 1300°F.

The FWT strength behavior of the Ti-14-21 specimens (low room temperature strength and high elevated temperature strength) can be related to the damage tolerance of the joint. The Pro-4 process most likely embrittled the Ti-14-21 honeycomb in the vicinity of the diffusion bonded joint (as was seen with the face sheet tensile specimens). Poor damage tolerance characteristics of the joint at room temperature resulted in failure at low FWT stress levels. At the elevated temperatures, the joint became more ductile and

more damage tolerant, allowing higher FWT stress levels to be attained prior to specimen fracture.

Figure 20 shows representative failure modes for Ti-14-21 honeycomb core FWT specimens tested at room temperature, 1200°F, 1300°F, and 1500°F. At room temperature, failure occurred at the interface between the face sheet and honeycomb core. At the elevated test temperatures, the failure location tended to move into the honeycomb core, resulting in more honeycomb core "stubble" remaining attached to the face sheet. However, the failure still occurred within the TLP-transformed portion of the honeycomb core adjacent to the diffusion bonded joint. The Ti-3-2.5, Ti-6-4, and Ti-15-3 honeycomb core FWT specimens exhibited failure modes similar to the Ti-14-21 specimens.

Edgewise Compression Tests

The average room and elevated temperature EWC strength data for the LID- and Pro-4-processed honeycomb core sandwich specimens are shown in figure 21. A complete tabulation of the EWC test data is shown in Appendix C. In all cases, the EWC strength decreased with increasing temperature. The Ti-3-2.5, Ti-6-4, and Ti-14-21 honeycomb core specimens exhibited similar EWC strengths up to 1100°F. Above 1100°F, the EWC strength of the Ti-3-2.5 and Ti-6-4 honeycomb core specimens decreased more rapidly with temperature than did that of the Ti-14-21 specimens. The Ti-15-3 honeycomb core specimens exhibited significantly higher EWC strength at room temperature and 1000°F than did the other three types of honeycomb core sandwich specimens. These higher EWC strengths were attributed to the higher face sheet/core joint strengths for the Ti-15-3 honeycomb core panel, as was previously shown with the FWT data in figure 19. Above 1000°F, the EWC strengths of the Ti-15-3 and Ti-14-21 specimens were similar.

Several failure modes are possible for sandwich structure tested in edgewise compression. The specimen can fail by face sheet wrinkling where the face sheets buckle into the core or tear away from the core in a symmetrical or anti-symmetric pattern. The specimen can also fail by shear crimping where the core fails by shear and the core and face sheets are displaced laterally together. If the face sheet-to-core bond is sufficiently strong, the face sheets can wrinkle and cause tensile failure of the core.

Figure 22 shows representative failure modes for Ti-3-2.5 honeycomb core EWC specimens tested at room temperature, 800°F, 1000°F, and 1100°F. At room temperature, the specimen failed by face sheet wrinkling as localized regions of the face sheets separated from the honeycomb core, resulting in symmetric outward buckling of the unsupported face sheets. At the elevated test temperatures, the joint between the face sheet and core was strong enough to preclude outward buckling of the face sheets. These specimens typically failed by shear crimping of the honeycomb core with the joint remaining intact. The Ti-6-4 and Ti-15-3 honeycomb core EWC specimens exhibited failure modes similar to those of the Ti-3-2.5 specimens at each temperature.

Figure 23 shows representative failure modes for Ti-14-21 honeycomb core EWC specimens tested at room temperature, 1000°F, and 1500°F. At room temperature, the specimen failed by face sheet wrinkling as localized regions of the face sheets separated from the honeycomb core and the unsupported face sheets buckled. Due to the limited room temperature ductility of the Pro-4-processed Ti-14-21, both the face sheet and honeycomb core fractured during the buckling deflection. At 1000°F, all of the specimens failed by face sheet wrinkling. At 1200°F and 1300°F, no consistent failure mode was observed. Some specimens failed by face sheet wrinkling while other specimens failed by shear crimping. All of

the specimens tested at 1500°F failed by shear crimping without joint failure. Thus, the general trend for all four types of honeycomb core EWC sandwich specimens was for joint failure and face sheet wrinkling to occur at room temperature and transition to shear crimping without failure of the joint at the elevated test temperatures.

The function of the core and bonded joint is to stabilize the face sheets in edgewise compression and to prevent localized buckling of the face sheets. The desired result of the EWC test is to develop full face sheet compressive yield properties. Figure 24 shows the room temperature and 1200°F compressive stress-strain curves for LID-processed Ti-3-2.5 honeycomb core EWC specimens. Also shown are the room temperature and 1200°F tensile stress-strain curves for the LID-processed Ti-14-21 face sheets. (Because sheet material cannot be effectively tested in compression, the face sheet compressive stress-strain curves are represented by tensile stress-strain curves. For most metals, the compressive properties are assumed to be slightly higher than the tensile properties based upon fracture mechanics principles.) The test results show good correlation between the EWC and tensile stress-strain curves and that the EWC specimens did not fail prior to face sheet yielding. These results indicate that the honeycomb cores and diffusion bonded joints were able to stabilize the face sheets up to or beyond the face sheet YS. These results were typical for all honeycomb core sandwich specimens and temperatures investigated.

The good correlation between EWC strength and face sheet yield strength for each honeycomb core sandwich at each temperature evaluated indicates the inherent structural integrity of these panels. The honeycomb cores and diffusion bonded joints were sufficiently strong to prevent specimen buckling failure prior to face sheet yielding. Once the EWC strength exceeded the face sheet yield strength, the failure mode was dictated by the relative strength levels of the honeycomb core and diffusion bonded joints.

Conclusions

This study was conducted to evaluate the suitability of transient liquid phase (TLP) bonding to fabricate titanium honeycomb core sandwich panels with Ti-14-21 titanium aluminide face sheets. Three titanium alloy honeycomb cores (Ti-3-2.5, Ti-6-4, and Ti-15-3) and one titanium aluminide alloy honeycomb core (Ti-14-21) were evaluated. Structural properties of the honeycomb core sandwich panels were determined using edgewise compression tests and the strength of the joint between the face sheet and honeycomb core was evaluated using flatwise tension tests. In addition, tensile tests were conducted on the Ti-14-21 face sheet material to determine the effects of processing on the face sheet properties. Tests were conducted at temperatures ranging from room temperature to 1500°F.

The two TLP processes that were evaluated (LID and Pro-4) produced well-diffused joints with large fillets at the face sheet/core nodes. No deleterious erosion of the foil gage honeycomb core was observed. The joint microstructures were characterized by a fine multiphase structure. The side of the face sheets to which the filler metals had been applied was transformed from equiaxed α_2 grains to coarse plates of α_2 with intergranular β. This transformed region was due to the β-stabilizing elements contained within the filler metal diffusing into the face sheets. Due to the higher temperature and longer time associated with the Pro-4 process compared to the LID process, diffusion occurred to a greater extent and the Pro-4-transformed region extended farther into the face sheet than did the LID-transformed region.

Tensile tests showed that LID-processing of the Ti-14-21 face sheet material caused a decrease in room temperature tensile and yield strength, an increase in modulus, and a minor decrease in ductility in comparison to unprocessed Ti-14-21 sheet tensile properties. The Pro-4-processed face sheets showed the same yield strength and

modulus trends as did the LID-processed face sheets. However, Pro-4 processing caused a significant reduction in room temperature face sheet ductility and UTS in comparison to the LID-processed face sheet tensile properties. Fractographic examination of the tensile specimens showed that this Pro-4-transformed region of the microstructure was dominated by brittle fracture. This embrittled region, which comprised approximately 20% of the face sheet cross-section, was most likely due to the greater depth of diffusion of filler metal elements into the Pro-4-processed face sheets than was observed in the LID-processed face sheets. This embrittlement could potentially be reduced by lowering the processing temperature and time and minimizing the amount of filler metal used to fabricate the panel.

Flatwise tension tests indicated that the Ti-15-3 specimens had the highest FWT strengths at temperatures up to 1000°F. At temperatures above 1000°F, the Ti-14-21 specimens had the highest FWT strengths. For all specimens tested, failure occurred in the vicinity of the diffusion bonded joint.

Edgewise compression tests indicated that the honeycomb cores and diffusion bonded joints were able to stabilize the face sheets up to or beyond the face sheet compressive yield strength for all temperatures investigated. After the face sheets yielded, failure occurred at room temperature by face sheet wrinkling as the joints failed, resulting in the outward buckling of the unsupported face sheets. As the temperature was increased, the failure mode transitioned to shear crimping with the joints remaining intact and shear failure of the core.

The non-optimized TLP bonding processes evaluated in this study produced sandwich panels with face sheet/honeycomb core joints strong enough to maintain structural integrity under compressive loading conditions at temperatures up to 1500°F. For incorporation into a hypersonic vehicle structure, the processing conditions would need to be optimized to tailor the honeycomb core sandwich properties for the loading conditions and flight environment associated with that particular structure. In addition, extensive evaluation of the damage tolerance and fatigue behavior of the TLP-bonded structure would need to be conducted. However, the results from this study indicate that TLP bonding has good potential for fabricating lightweight honeycomb core sandwich structure with titanium aluminide face sheets and titanium aluminide or conventional titanium alloy honeycomb core suitable for high-temperature hypersonic vehicle applications.

References

1. Tenney, D.R.; Lisagor, W.B.; Dixon, S.C.: Materials and Structures for Hypersonic Vehicles. NASA Technical Memorandum 101501, October 1988.

2. Sorensen, J.P. and Smith, P.R.: Titanium Matrix Composites for the National Aerospace Plane. *Proceedings of the 13th Conference on Metal Matrix, Carbon, and Ceramic Matrix Composites.* NASA Conference Proceedings 3054, Part 2, pp. 569–581, 1990.

3. Froes, F.H.: Advances in Lightweight Metallic Materials for Aerospace Applications. *Proceedings of the 2nd International SAMPE Metals and Metals Processing Conference*. Volume 2: Space Age Metals Technology, F.H. Froes and R.A. Cull, eds., pp. 1–19, 1988.

4. Larsen, J.M.; Williams, K.A.; Balsone, S.J.; Stucke, M.A.: Titanium Aluminides for Aerospace Applications. *High Temperature Aluminides and Intermetallics*. C.T. Liu, et al, eds., TMS/ASM International, USA, 1990.

5. Lipsitt, H.A.: Titanium Aluminides - An Overview. *Materials Research Society Symposium Proceedings*. Volume 39. Materials Research Society, 1985.

6. Sastry, S.M.L.; Lipsitt, H.A.: Plastic Deformation of TiAl and Ti_3Al. *Proceedings of the 4th International Conference on Titanium*, Japan, pp. 1231–1243, 1980.

7. Woodward, J.R.: Liquid Interface Diffusion Method of Bonding Titanium and/or Titanium Alloy Structure. U.S. Patent 3,957,194, May 18, 1976.

8. Woodward, J.R.: Liquid Interface Diffusion Method of Bonding Titanium and/or Titanium Alloy Structure and Product Using Nickel-copper, Silver Bridging Material. U.S. Patent 3,854,194, December 17, 1974.

9. Woodward, J.R.: Liquid Interface Diffusion Method of Bonding Titanium and Titanium Alloy Honeycomb Sandwich Panel Structure. U.S. Patent 3,769,101, October 30, 1973.

10. Woodward, J.R.: Liquid Interface Diffusion Bonded Titanium. U.S. Patent 3,768,985, October 30, 1973.

11. Norris, B.: Liquid Interface Diffusion (LID) Bonding of Titanium Structures. Proceedings of the International Conference on "Designing with Titanium," University of Bristol, United Kingdom, July 7–9, 1986.

12. Norris, B; Gojny, F.: Joining Processes Used in the Fabrication of Titanium and Inconel Honeycomb Sandwich Structures. First International SAMPE Metals and Metals Processing Conference, Cherry Hill, New Jersey, August 18–20, 1987.

13. Standard Test Methods of Tension Testing of Metallic Materials; Designation E8-91. Annual Book of ASTM Standards, Vol 03.01. American Society for Testing and Materials, 1992, pp. 130–146.

14. Standard Test Method of Tension Test of Flat Sandwich Constructions in Flatwise Plane; Designation C297-61. Annual Book of ASTM Standards, Vol 15.03. American Society for Testing and Materials, 1984, pp. 12–14.

15. Standard Test Method for Edgewise Compression Strength of Flat Sandwich Constructions; Designation C364-61. Annual Book of ASTM Standards, Vol 15.03. American Society for Testing and Materials, 1984, pp. 17–19.

16. Hoffman, Eric K.; Bird, R. Keith; and Dicus, Dennis L.: Effect of Braze Processing on the Microstructure and Mechanical Properties of SCS-6/b21S Titanium Matrix Composites. AIAA-92-5017, Dec. 1992.

Table 1. Description of Ti-14-21 based honeycomb core sandwich panels

	Panel Components			
	Ti-14-21 face sheets			
	Ti-3-2.5 core	Ti-6-4 core	Ti-15-3 core	Ti-14-21 core
Face sheet thickness (in)	0.020	0.020	0.020	0.020
Honeycomb core cell type	square, corrugated	square, corrugated	square, corrugated	square, corrugated
Honeycomb core cell size (in)	0.25	0.25	0.25	0.375
Honeycomb core cell wall thickness (in)	0.002	0.002	0.002	0.004
Honeycomb core height (in)	0.6	0.6	0.6	0.6
Filler metal	LID (Cu/Ni)	LID (Cu/Ni)	LID (Cu/Ni)	Pro-4 (Cu/Sn)
Panel length and width (in)	30×21	30×21	30×21	30×21
Panel weight (lb/ft^2)	1.07	1.11	1.26	1.33

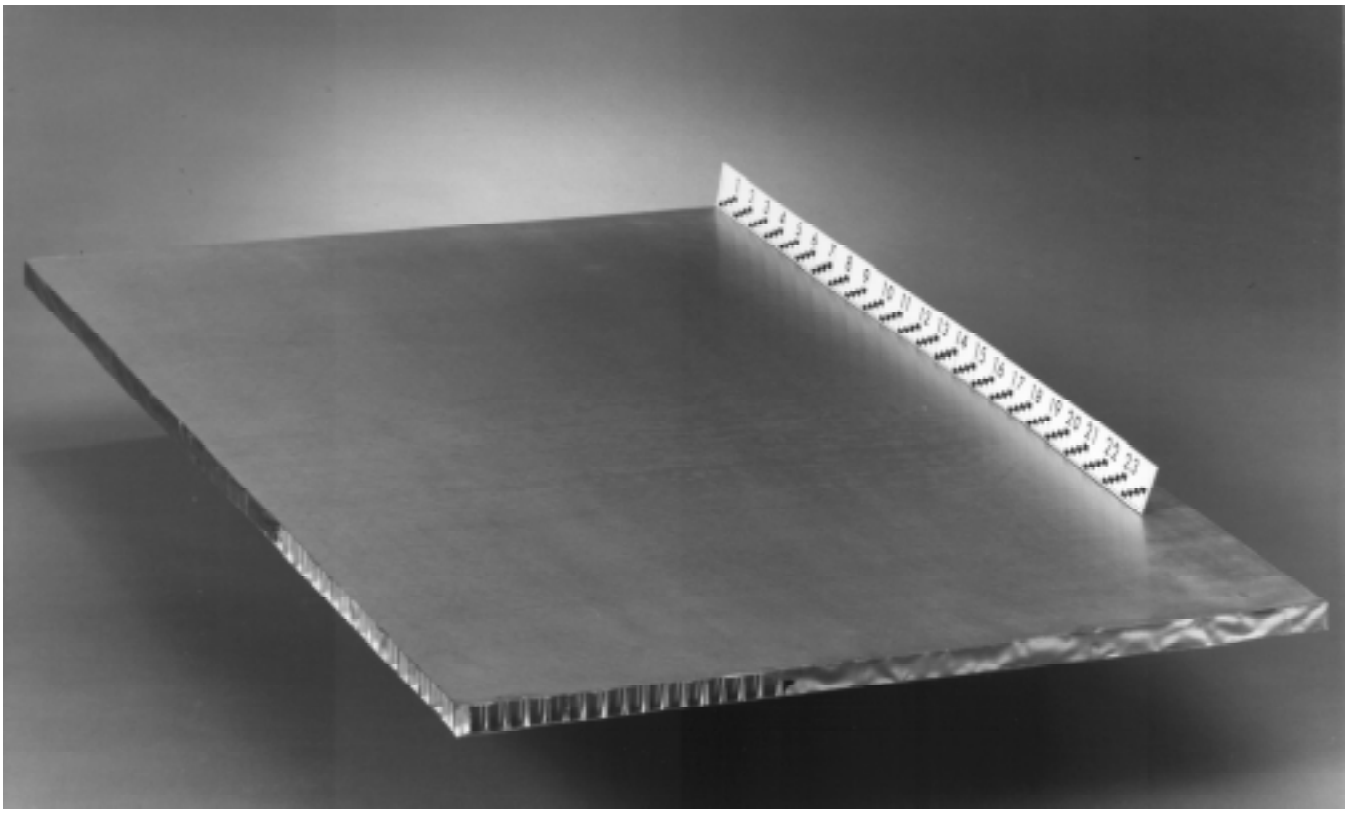

Figure 1. TLP bonded sandwich panel with Ti-14Al-21Nb face sheets and honeycomb core.

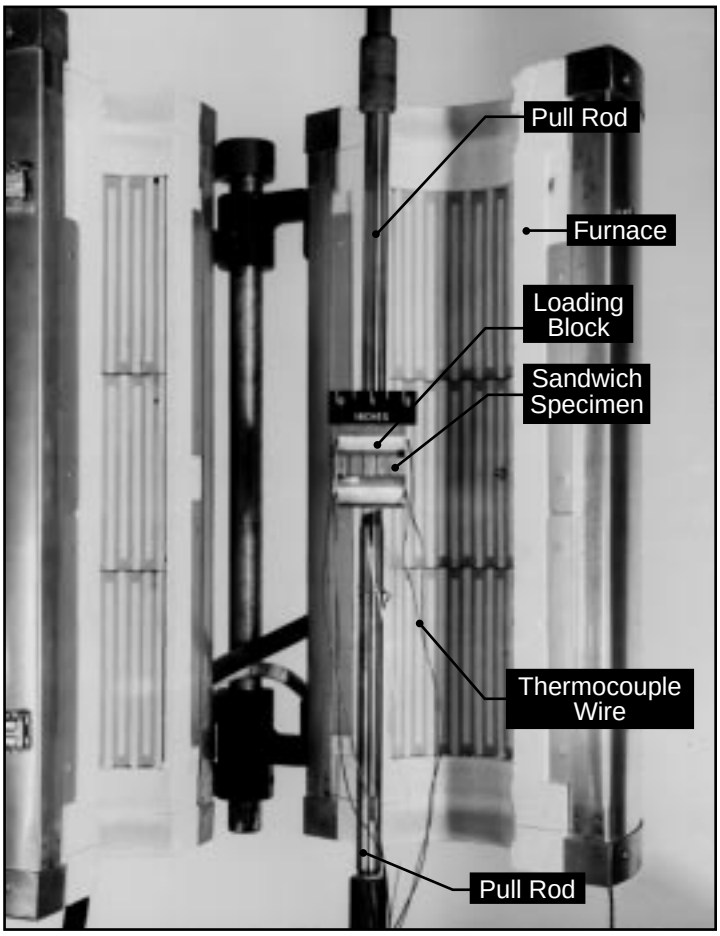

Figure 2. FWT test apparatus and specimen.

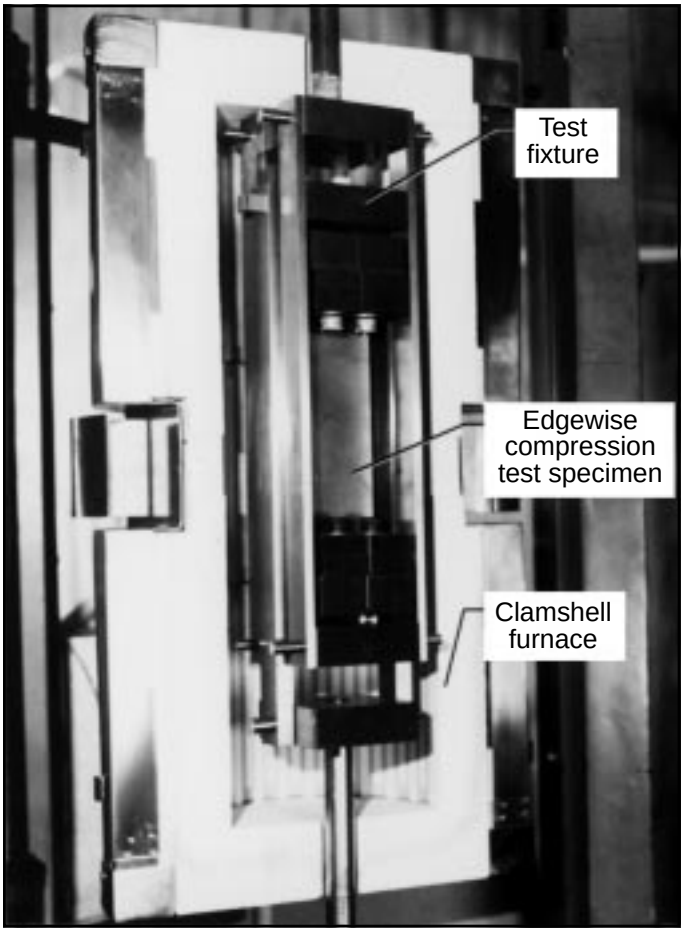

Figure 3. EWC test apparatus and specimen.

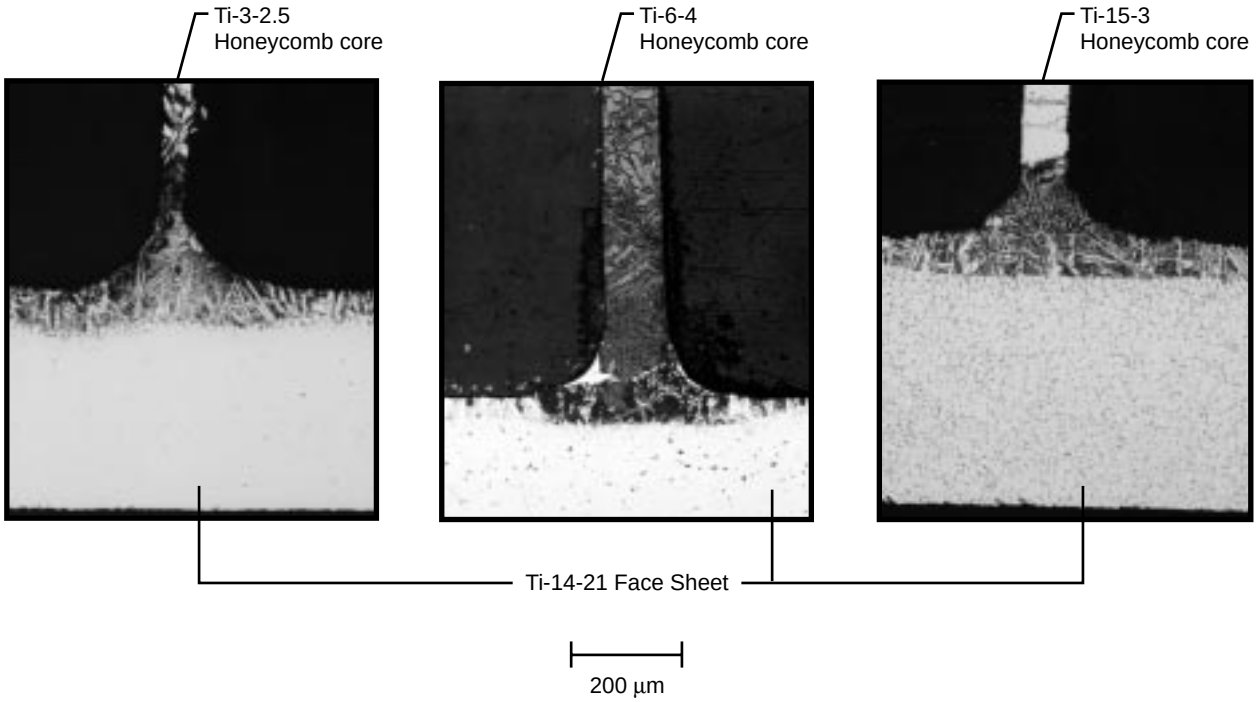

Figure 4. Microstructure of LID-processed honeycomb core sandwich panel joints.

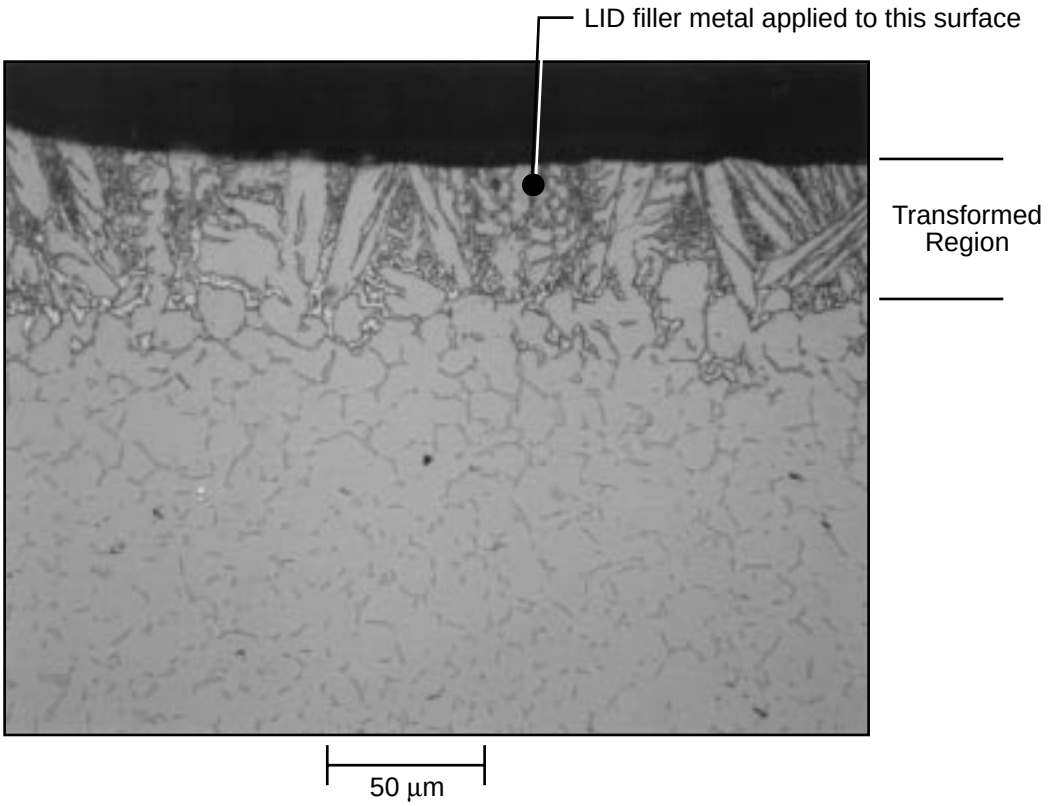

Figure 5. Microstructure of LID-processed Ti-14-21 face sheet remote from the joint.

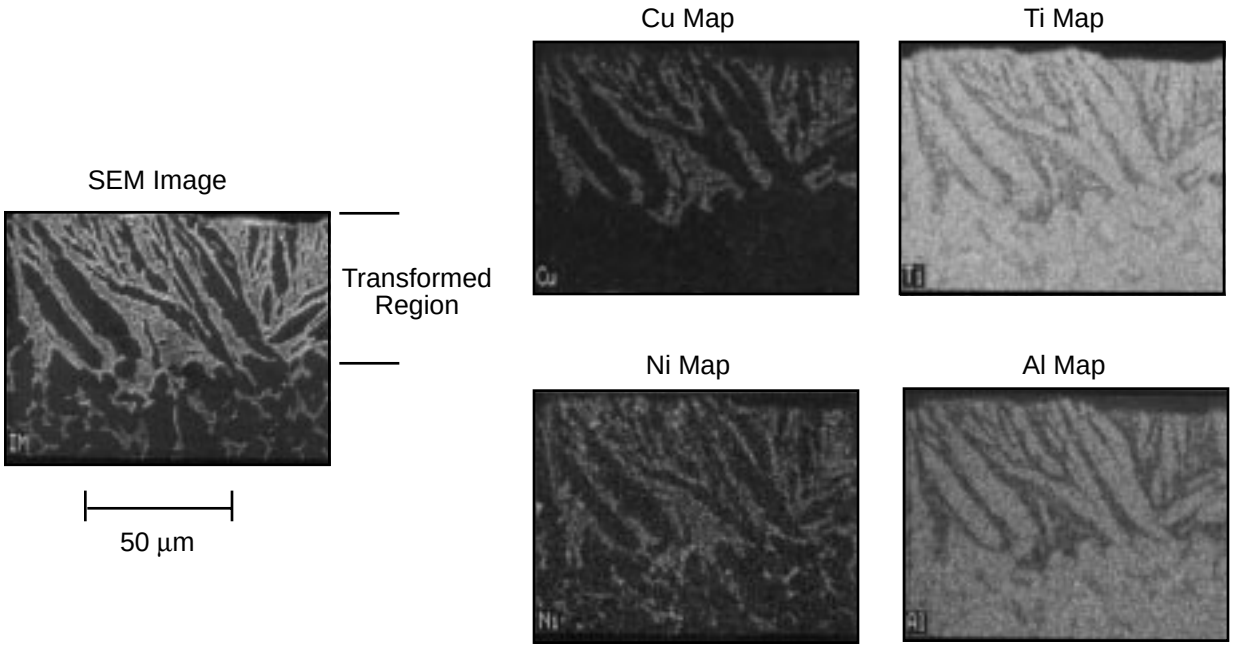

Figure 6. SEM image and EDS x-ray map of elements in LID-processed Ti-14-21 face sheet transformed region.

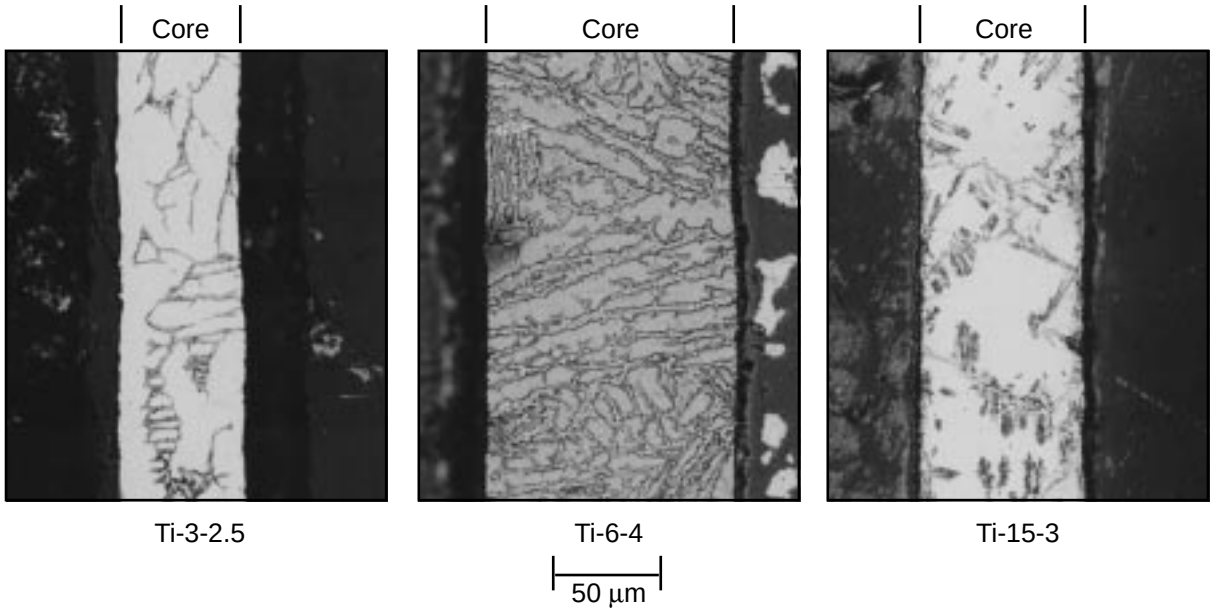

Figure 7. Microstructure of LID-processed honeycomb cores remote from the joint.

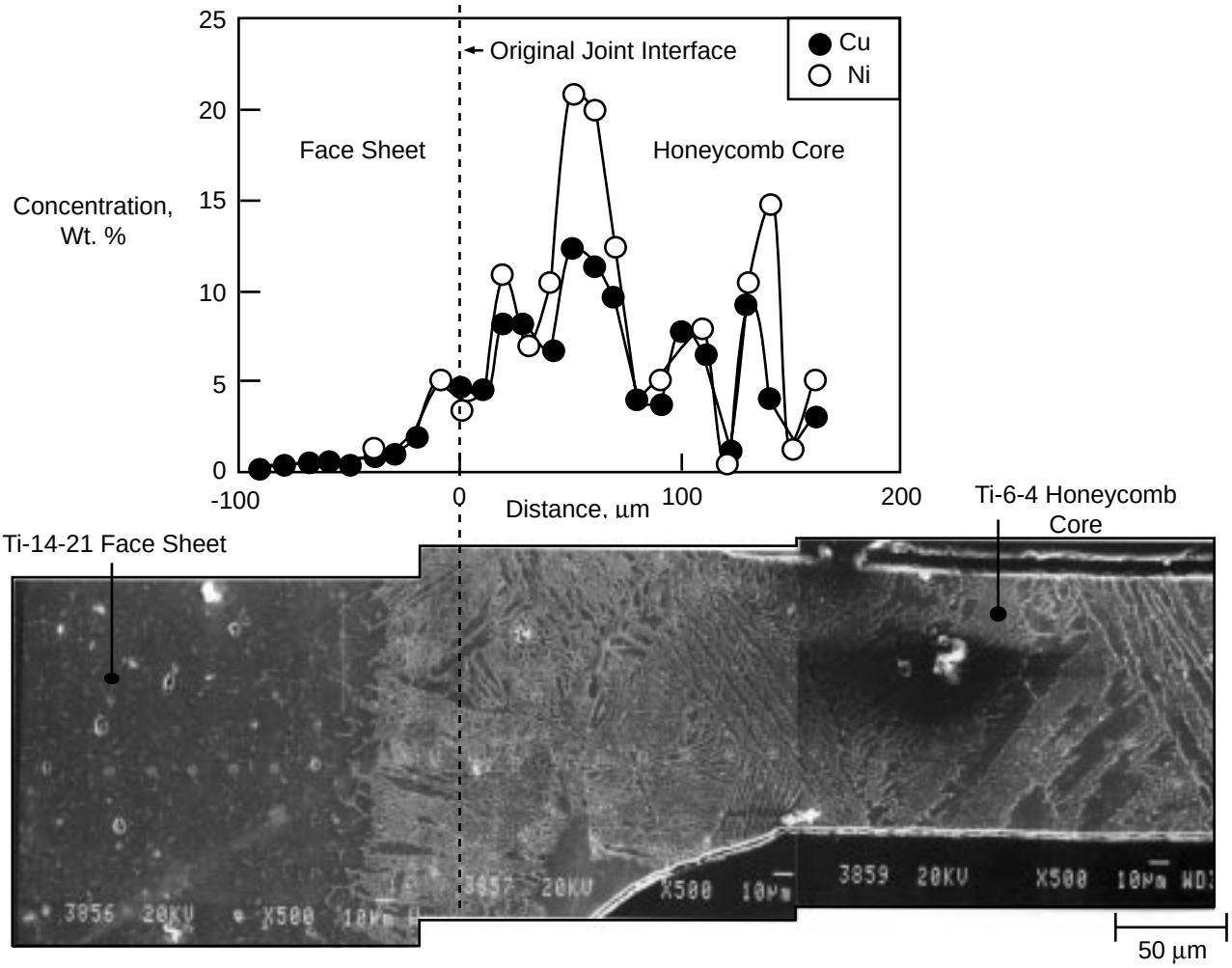

Figure 8. SEM image and WDS analysis of Cu and Ni concentration profiles across the joint interface in a LID-processed honeycomb core sandwich panel.

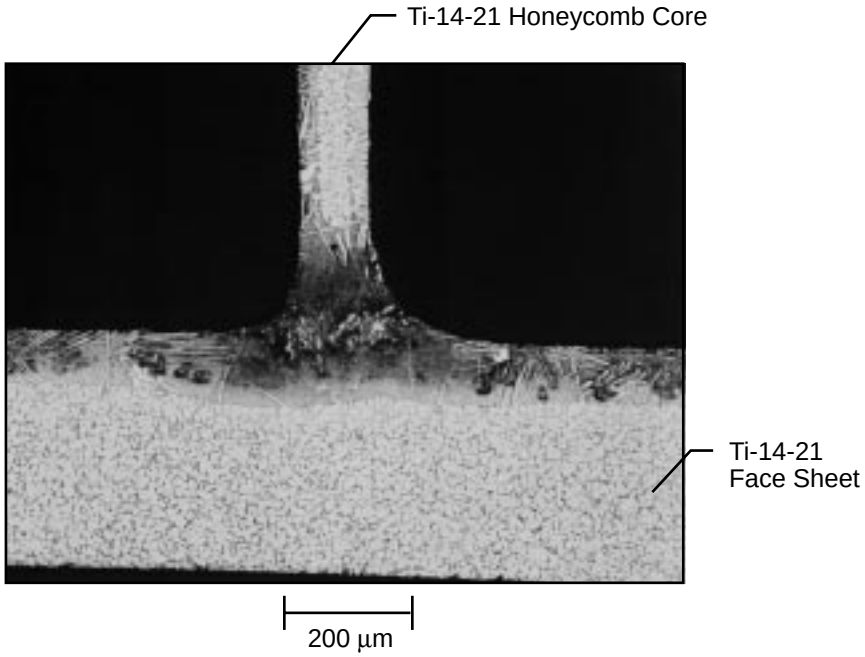

Figure 9. Microstructure of Pro-4-processed honeycomb core sandwich panel joint.

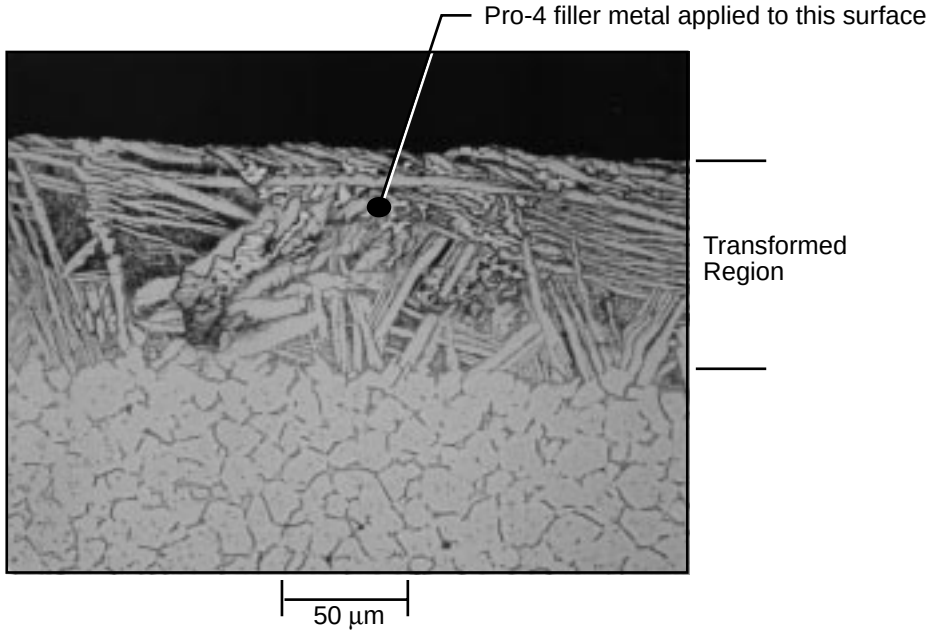

Figure 10. Microstructure of Pro-4-processed Ti-14-21 face sheet remote from the joint.

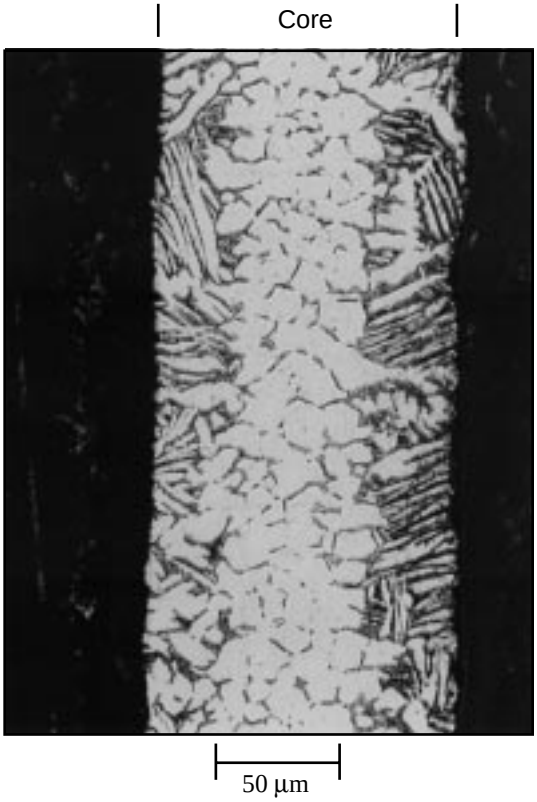

Figure 11. Microstructure of Pro-4-processed Ti-14-21 honeycomb core remote from the joint.

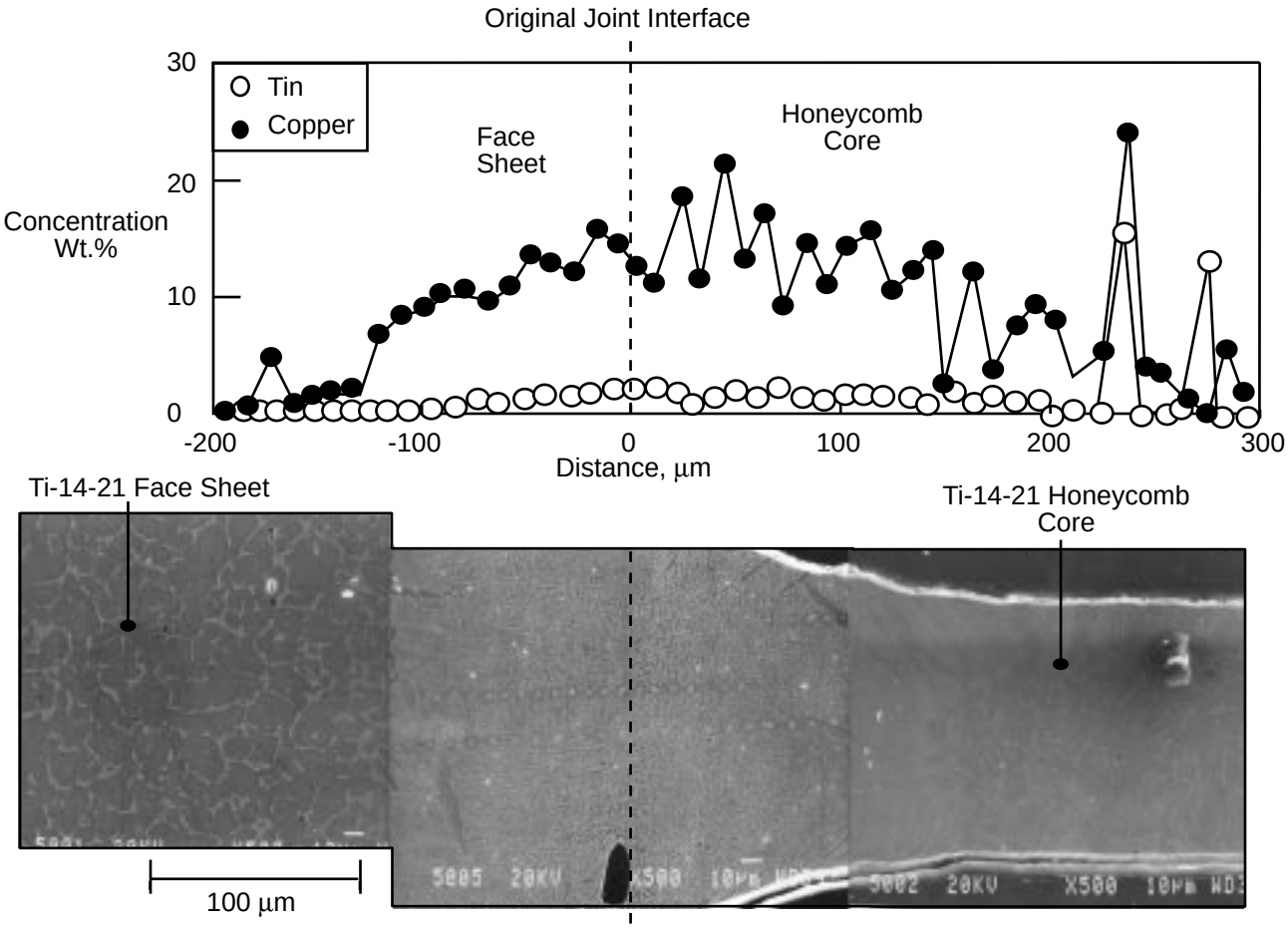

Figure 12. SEM image and WDS analysis of Cu and Sn concentration profile across the joint interface in a Pro-4-processed honeycomb core sandwich panel.

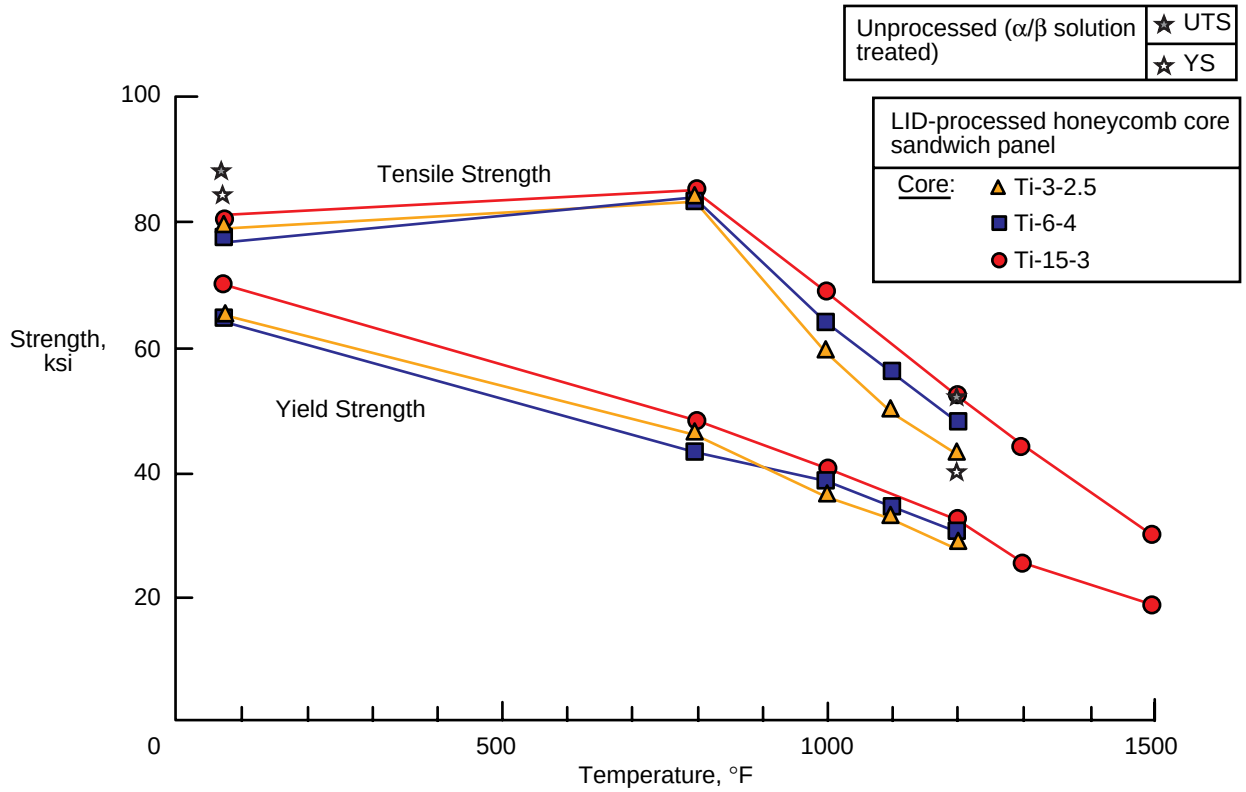

Figure 13. Effect of temperature on average strength of unprocessed and LID-processed Ti-14-21 face sheet material.

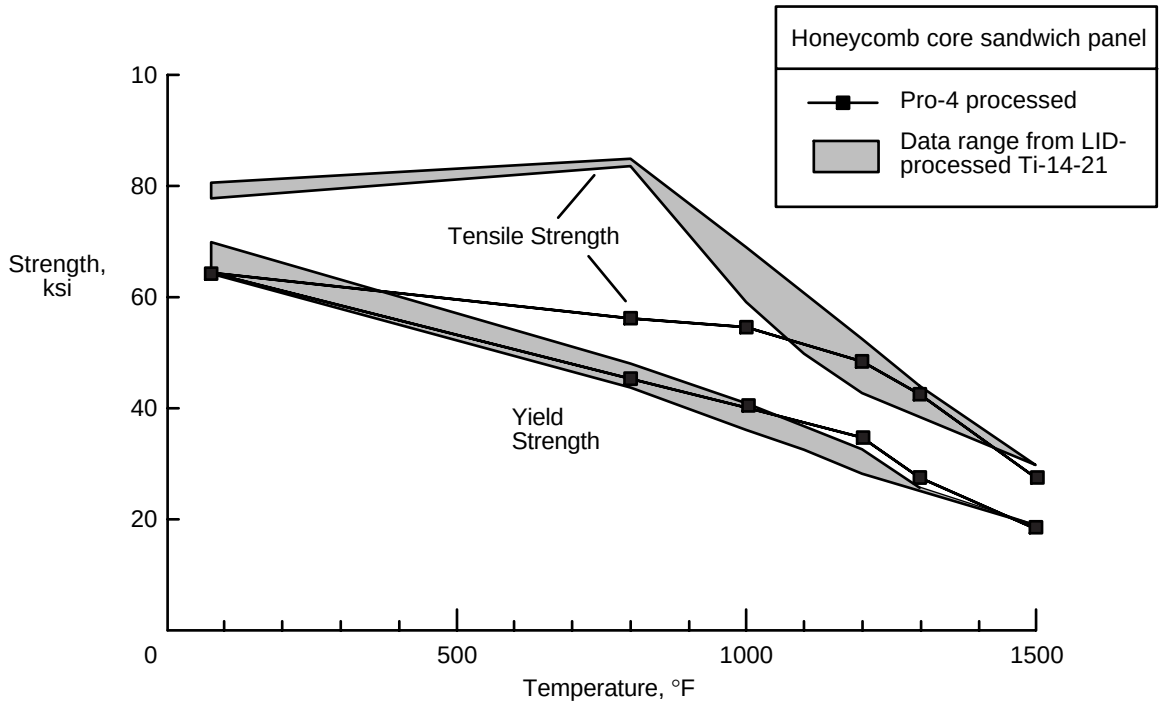

Figure 14. Effect of temperature on average strength of LID- and Pro-4-processed Ti-14-21 face sheet material.

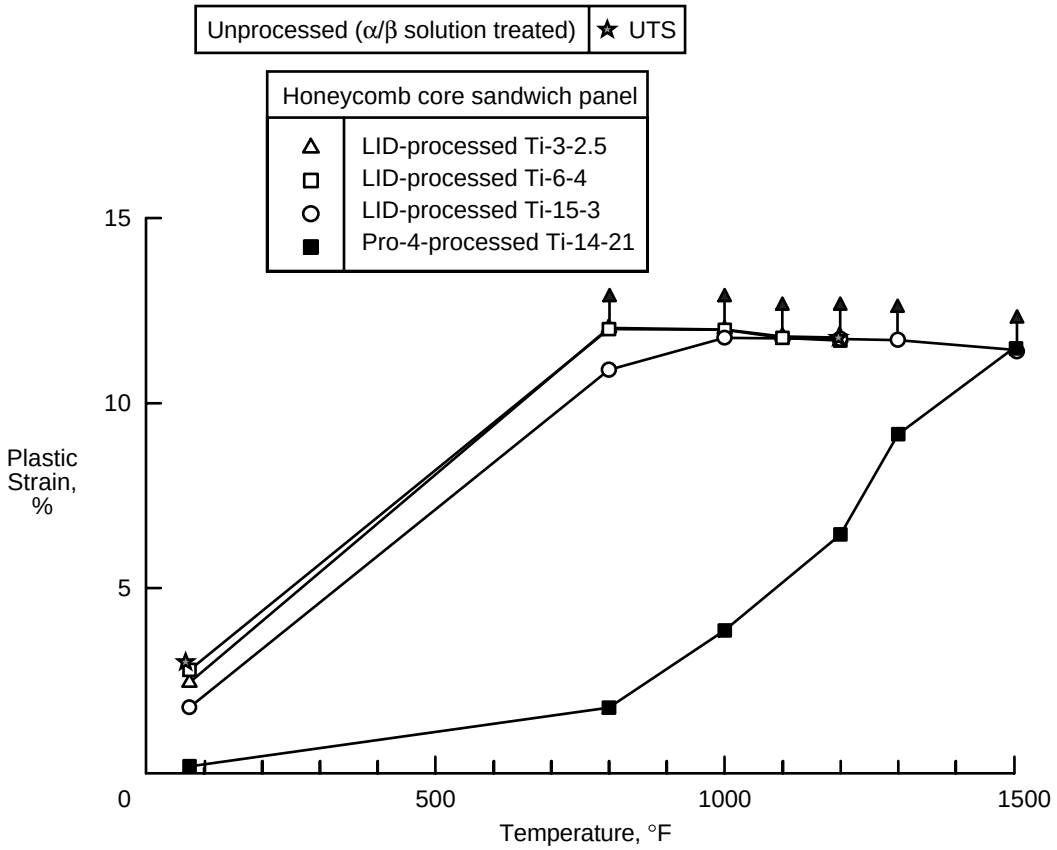

Figure 15. Effect of temperature on average ductility of unprocessed, LID-processed, and Pro-4-processed Ti-14-21 face sheet material.

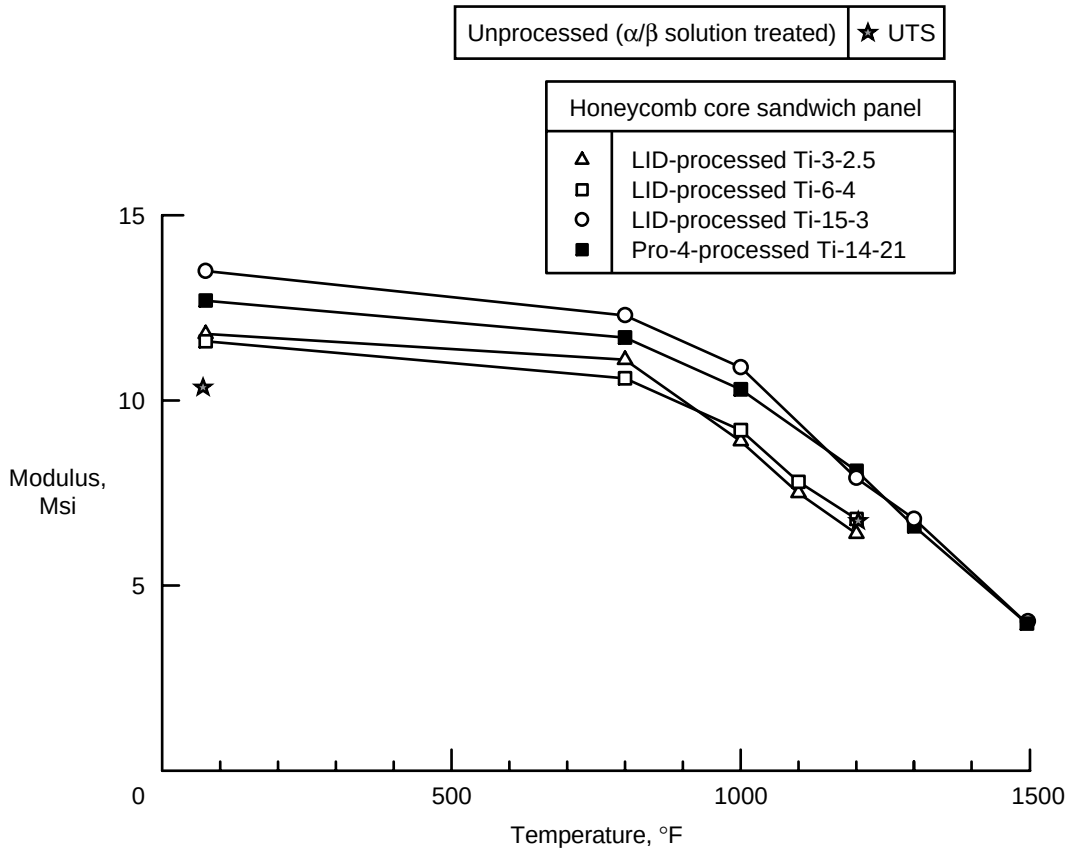

Figure 16. Effect of temperature on average modulus of unprocessed, LID-processed, and Pro-4-processed Ti-14-21 face sheet material.

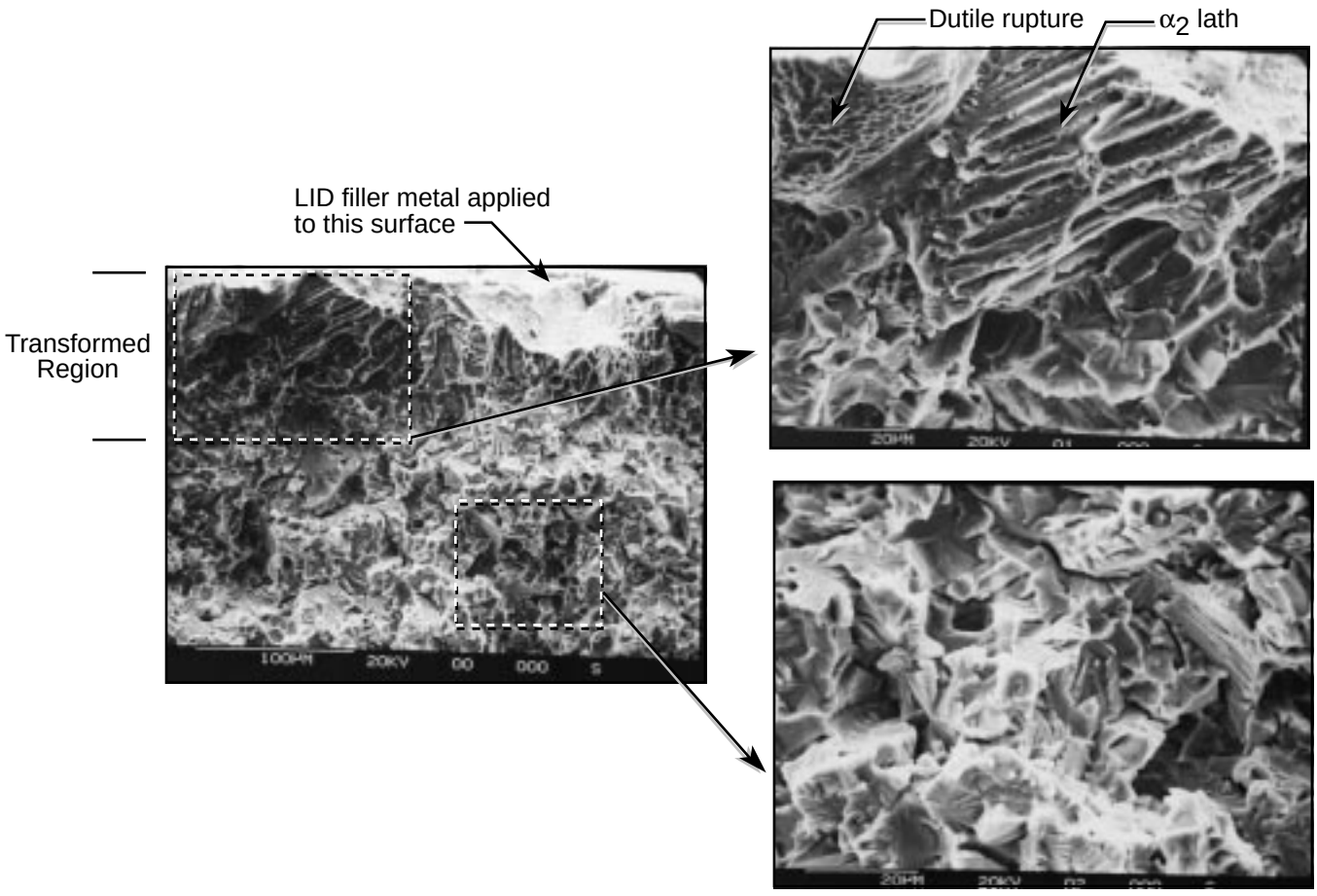

Figure 17. Room temperature fracture surface of LID-processed Ti-14-21 face sheet tensile specimen.

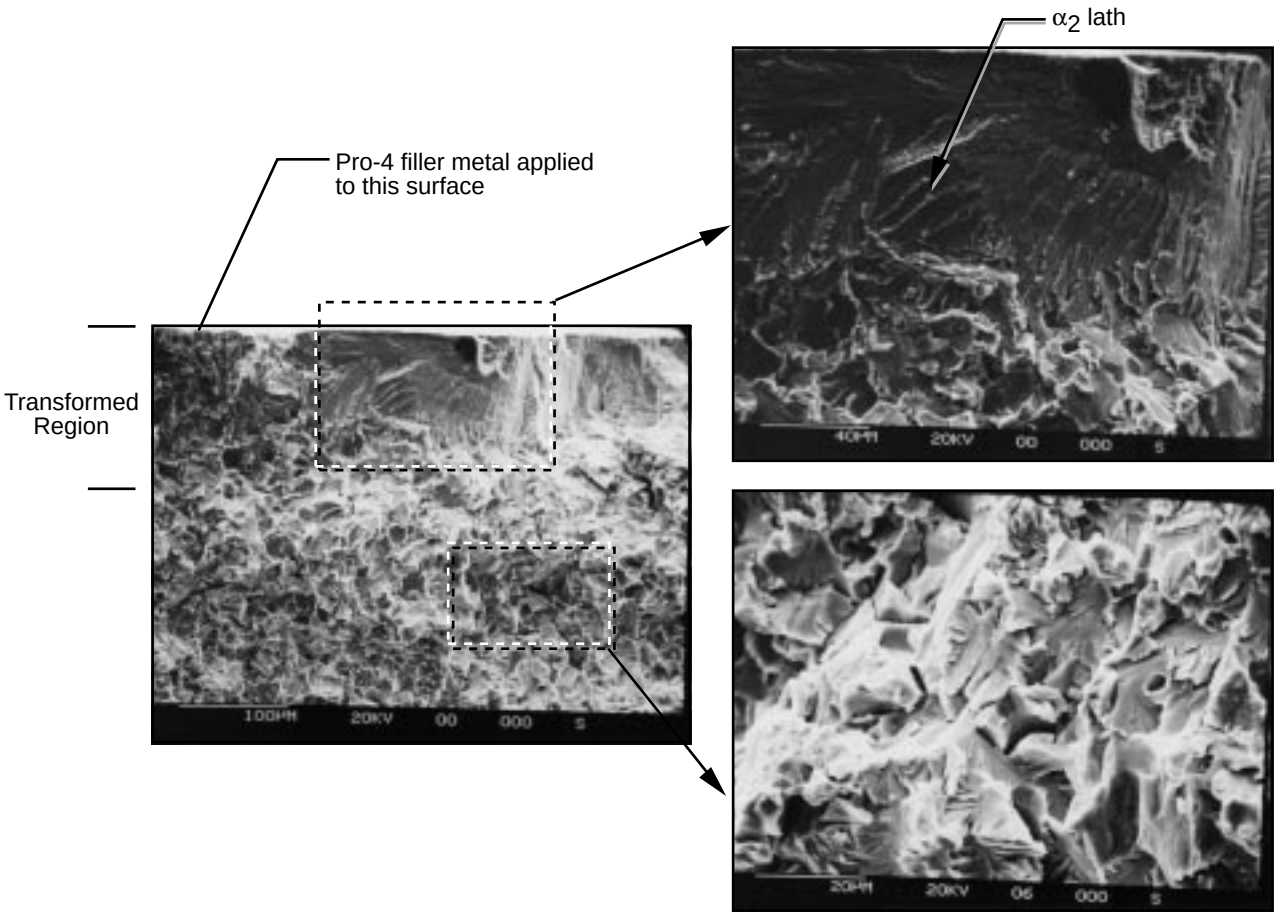

Figure 18. Room temperature fracture surface of Pro-4-processed Ti-14-21 face sheet tensile specimen.

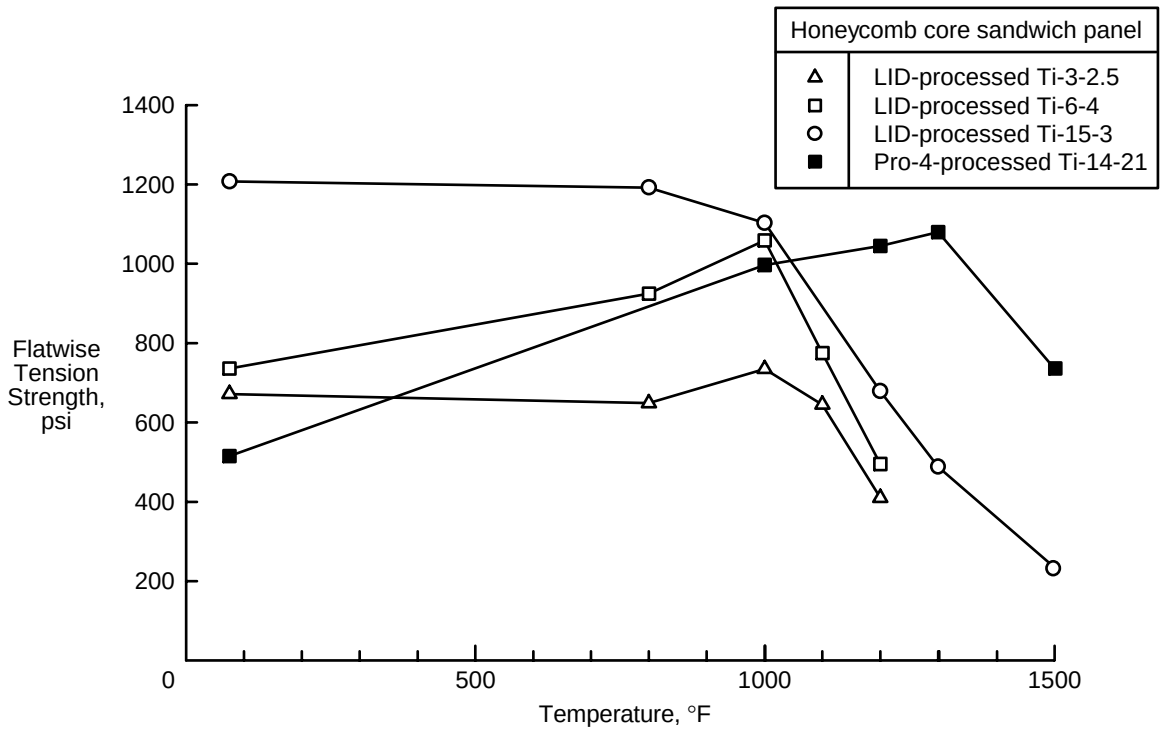

Figure 19. Effect of temperature on average FWT strength of LID- and Pro-4-processed honeycomb core sandwich specimens.

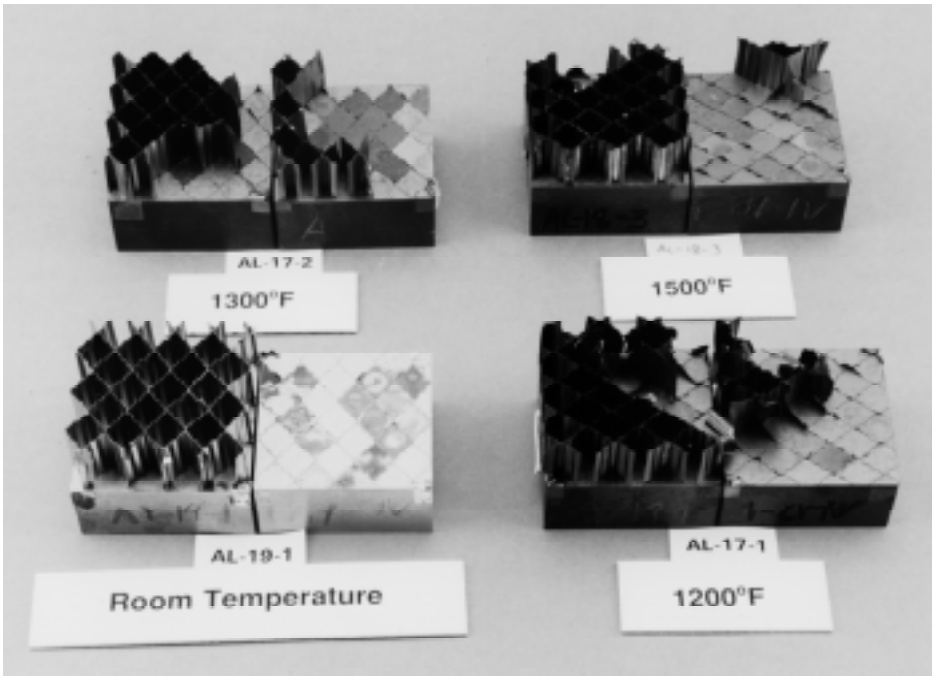

Figure 20. Room and elevated temperature failure modes for Ti-14-21 honeycomb core FWT specimens.

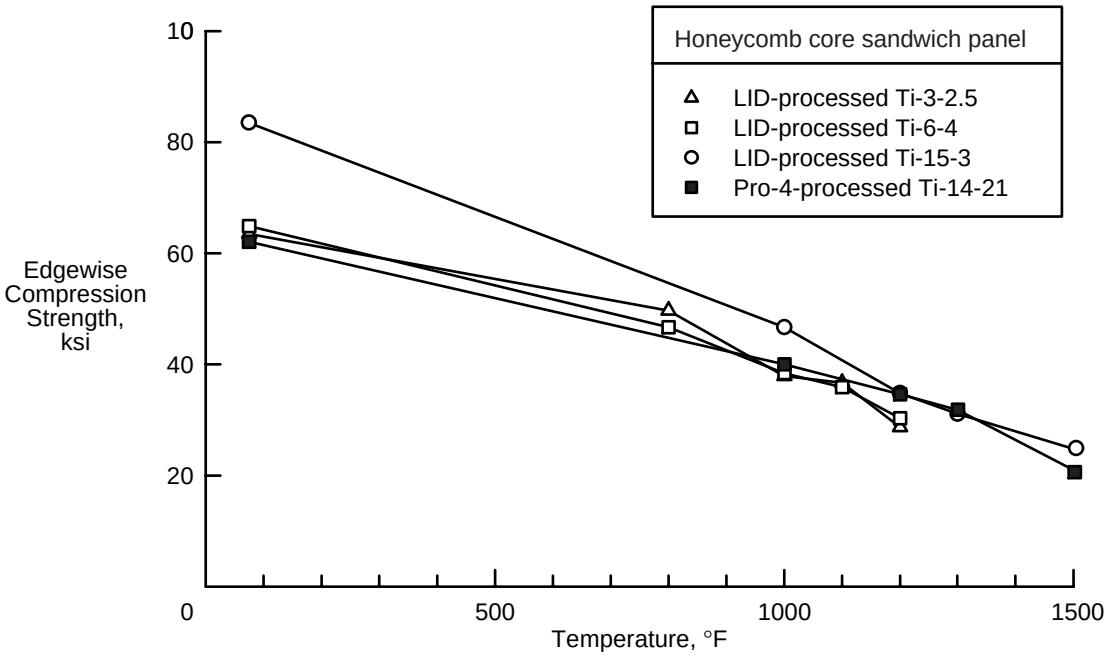

Figure 21. Effect of temperature on average EWC strength of LID- and Pro-4-processed honeycomb core sandwich specimens.

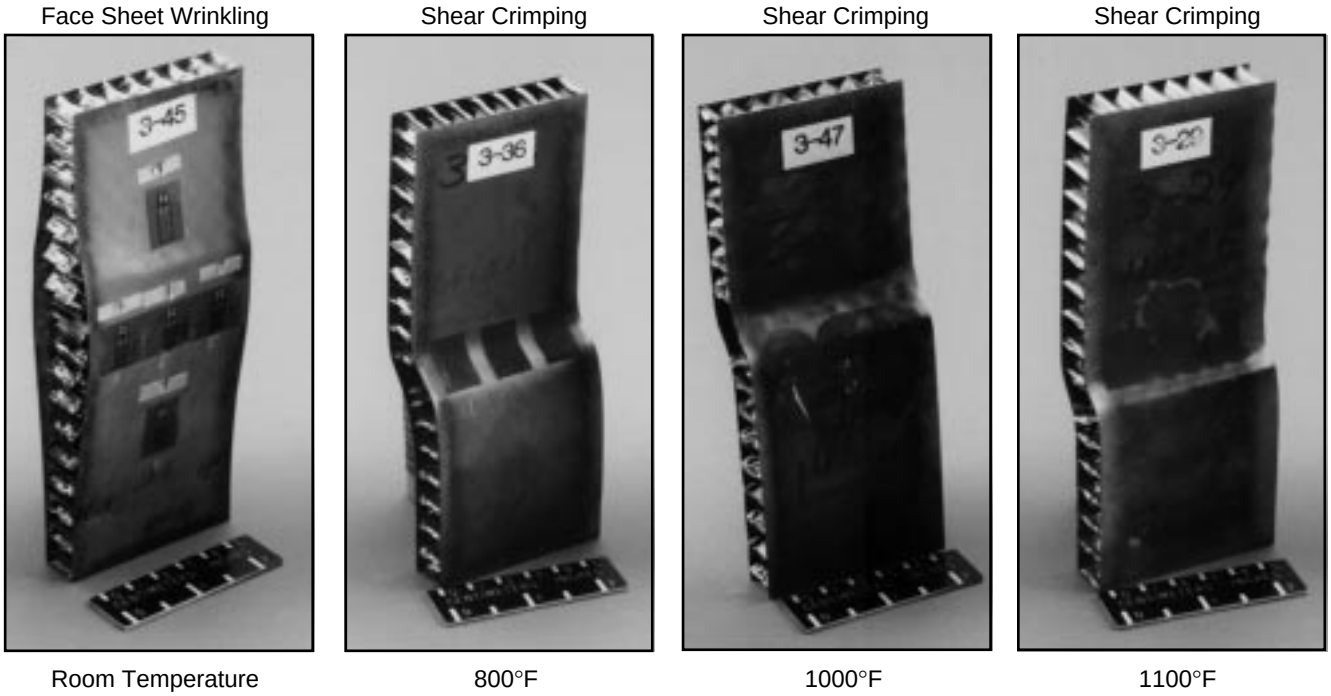

Figure 22. Room and elevated temperature failure modes for Ti-3-2.5 honeycomb core EWC specimens.

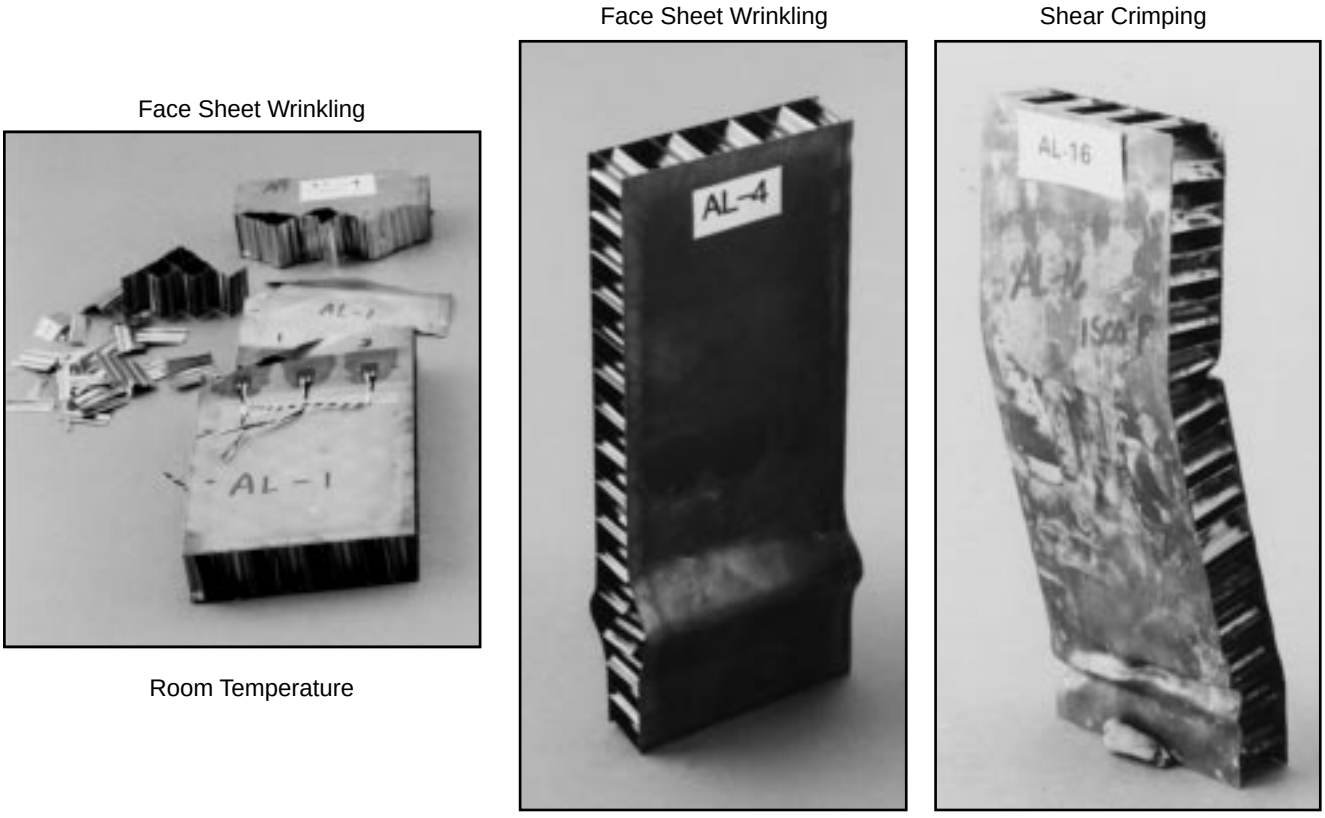

Figure 23. Room and elevated temperature failure modes for Ti-14-21 honeycomb core EWC specimens.

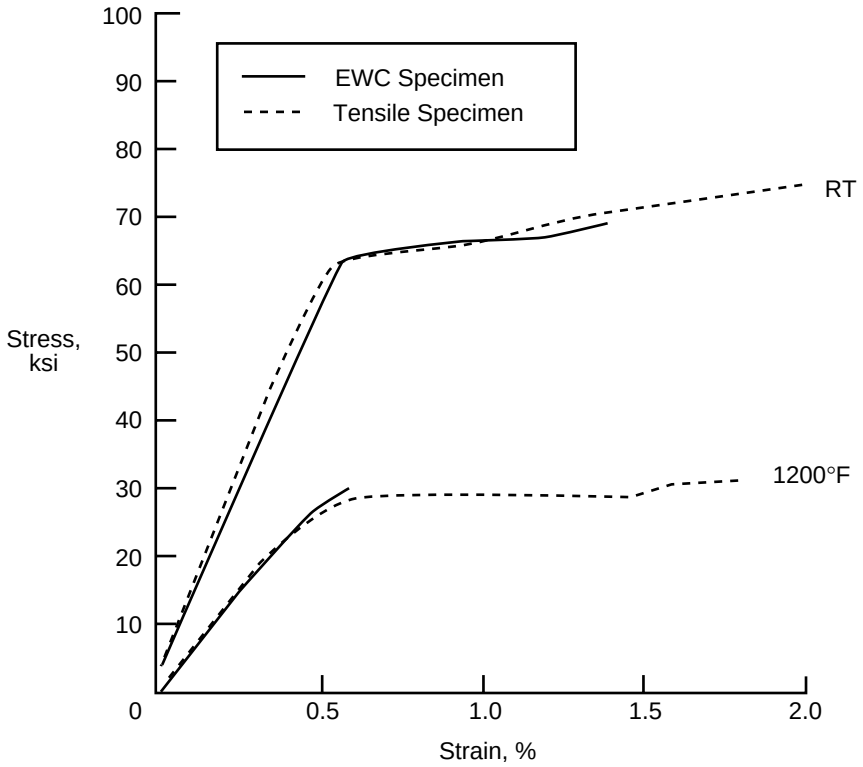

Figure 24. Room temperature and 1200°F stress-strain curves for LID-processed Ti-3-2.5 honeycomb core EWC specimens and Ti-14-21 face sheet tensile specimens.

Appendix A

Unprocessed, LID-Processed, and Pro-4-Processed Ti-14-21 Face Sheet Tensile Data

Table A-1. Tensile properties of unprocessed Ti-14-21 sheet material in the α/β solution treated condition

Specimen No.	Temp. (°F)	UTS (ksi)	YS (ksi)	E (Msi)	e_p (%)
U-1	Room Temp.	90.8	81.9	10.4	3.0
U-2	1200	51.0	40.0	7.0	>12[a]

[a]Specimen did not fail. Test stopped after this amount of plastic strain.

Table A-2. Tensile properties of Ti-14-21 face sheet material from LID-processed Ti-3-2.5 honeycomb core sandwich panel

Specimen No.	Temp.(°F)	UTS (ksi)	YS (ksi)	E (Msi)	e_p (%)
3-41-1	Room Temp.	80.3	64.7	11.9	2.51
3-41-2		81.2	64.5	11.8	2.77
3-41-3		80.2	63.7	11.7	2.59
3-41-4		77.5	63.9	11.7	1.92
3-41-5	800	84.0	46.2	11.3	12.04
3-41-6		83.6	45.8	10.9	12.01
3-41-7	1000	58.9	35.9	8.6	>12.12[a]
3-41-8		59.2	36.2	9.1	>11.85[a]
3-41-9	1100	49.4	32.3	7.6	>11.80[a]
3-41-10		50.2	32.6	7.4	>11.80[a]
3-41-11	1200	43.1	28.4	6.6	>11.81[a]
3-41-12		42.3	28.0	6.2	>11.72[a]

[a]Specimen did not fail. Test stopped after this amount of plastic strain.

Table A-3. Tensile properties of Ti-14-21 face sheet material from LID-processed Ti-6-4 honeycomb core sandwich panel

Specimen No.	Temp. (°F)	UTS (ksi)	YS (ksi)	E (Msi)	e_p (%)
6-33-7	Room Temp.	76.9	64.9	11.7	2.72
6-33-8		77.3	65.3	11.5	2.53
6-33-9		78.3	65.5	11.5	3.09
6-33-10		78.6	64.5	11.7	2.82
6-33-11	800	79.1	44.1	11.0	>12.04[a]
6-33-12		88.1	43.2	10.2	>18.03[a]
6-34-13	1000	64.4	38.3	9.3	>12.10[a]
6-34-14		64.0	38.2	9.1	>11.85[a]
6-34-15	1100	55.7	34.2	7.8	>11.78[a]
6-34-16		56.6	34.9	7.8	>11.74[a]
6-34-17	1200	48.0	30.7	6.9	>11.72[a]
6-34-18		48.2	30.9	6.6	>11.66[a]

[a]Specimen did not fail. Test stopped after this amount of plastic strain.

Table A-4. Tensile properties of Ti-14-21 face sheet material from LID-processed Ti-15-3 honeycomb core sandwich panel

Specimen No.	Temp. (°F)	UTS (ksi)	YS (ksi)	E (Msi)	e_p (%)
15-41-1	Room Temp.	82.5	70.0	13.7	2.09
15-41-2		78.3	69.3	13.0	1.50
15-41-3		78.5	70.1	13.7	1.33
15-41-4		83.2	70.0	13.5	2.21
15-41-5	800	83.4	48.1	12.6	9.75
15-41-6		86.4	47.8	12.0	>12.05[a]
15-41-7	1000	67.3	41.1	10.9	11.63
15-41-8		70.6	40.7	10.9	>11.88[a]
15-41-9	1200	52.1	32.5	7.9	>11.72[a]
15-41-10		52.9	32.7	7.8	>11.73[a]
15-41-11	1300	43.9	25.4	6.9	>11.74[a]
15-41-12		44.1	25.9	6.7	>11.66[a]
15-42-13	1500	29.5	19.0	3.8	>11.42[a]
15-42-14		30.1	18.8	4.1	>11.46[a]

[a]Specimen did not fail. Test stopped after this amount of plastic strain.

Table A-5. Tensile properties of Ti-14-21 face sheet material from Pro-4-processed Ti-14-21 honeycomb core sandwich panel

Specimen No.	Temp. (°F)	UTS (ksi)	YS (ksi)	E (Msi)	e_p (%)
AL-11-1	Room Temp.	64.7	—[b]	12.8	0.19
AL-11-2		64.9	—[b]	12.6	0.18
AL-11-3		64.6	64.5	12.9	0.20
AL-11-4		63.3	—[b]	12.4	0.17
AL-11-5	800	58.5	45.3	11.9	2.06
AL-11-6		53.8	45.2	11.5	1.48
AL-11-8	1000	53.1	39.1	10.2	3.40
AL-11-9		56.0	41.0	10.4	4.32
AL-11-10	1200	47.0	34.5	8.1	5.64
AL-11-11		49.8	34.9	8.1	7.26
AL-11-12	1300	40.8	27.3	6.5	6.67
AL-12-13		44.2	27.7	6.6	>11.65[a]
AL-12-14	1500	27.5	18.0	4.1	>11.47[a]
AL-12-15		27.4	18.6	3.8	>11.51[a]

[a]Specimen did not fail. Test stopped after this amount of plastic strain.
[b]YS was not calculated because specimen did not attain 0.2% plastic strain.

Appendix B

Flatwise Tension Data for LID- and Pro-4-Processed Honeycomb Core Sandwich Panels

Table B-1. FWT strength of LID-processed Ti-3-2.5 honeycomb core sandwich specimens

Specimen No.	Temp. (°F)	FWT strength (psi)
3-2	Room Temp.	888
3-3		665
3-4		678
3-5		513
3-14		615
3-11	800	623
3-12		695
3-16		630
3-6	1000	715
3-7		808
3-8		650
3-9		765
3-20	1100	575
3-21		625
3-22		735
3-17	1200	390
3-18		368
3-19		473

Table B-2. FWT strength of LID-processed Ti-6-4 honeycomb core sandwich specimens

Specimen No.	Temp. (°F)	FWT strength (psi)
6-2	Room Temp.	803
6-3		713
6-6		693
6-4	800	890
6-5		895
6-9		990
6-10	1000	998
6-19		973
6-20		1205
6-13	1100	793
6-14		835
6-15		698
6-12	1200	395
6-21		478
6-22		613

Table B-3. FWT strength of LID-processed Ti-15-3 honeycomb core sandwich specimens

Specimen No.	Temp. (°F)	FWT strength (psi)
15-3	Room Temp.	1340
15-4		1038
15-5		1025
15-6		1430
15-16	800	1188
15-23		1050
15-24		1338
15-7	1000	985
15-8		1200
15-10		1050
15-11		1175
15-14	1200	615
15-15		648
15-19		775
15-17	1300	458
15-18		483
15-20		523
15-12	1500	225
15-13		188
15-21		295

Table B-4. FWT strength of Pro-4-processed Ti-14-21 honeycomb core sandwich specimens

Specimen No.	Temp.(°F)	FWT strength (psi)
AL-25	Room Temp.	704
AL-26		521
AL-27		694
AL-28		451
AL-36		483
AL-37		390
AL-39		423
AL-40		365
AL-19-1		605
AL-30	1000	968
AL-31		974
AL-32		1049
AL-45	1200	1110
AL-47		1075
AL-17-1		950
AL-48	1300	1060
AL-17-2		1113
AL-17-3		1068
AL-29	1500	853
AL-34		482
AL-43		892
AL-18-3		725

Appendix C

Edgewise Compression Data for LID- and Pro-4-Processed Honeycomb Core Sandwich Panels

Table C-1. EWC strength of LID-processed Ti-3-2.5 honeycomb core sandwich specimens

Specimen No.	Temp. (°F)	EWC strength (ksi)
3-26	Room Temp.	68.0
3-30		58.8
3-45		63.7
3-35	800	55.2
3-37		44.2
3-46	1000	40.9
3-47		37.2
3-48		35.7
3-28	1100	38.3
3-29		35.9
3-31		35.8
3-32	1200	29.8
3-43		28.3
3-44		27.9

Table C-2. EWC strength of LID-processed Ti-6-4 honeycomb core sandwich specimens

Specimen No.	Temp. (°F)	EWC strength (ksi)
6-25	Room Temp.	68.8
6-26		64.7
6-27		61.3
6-28	800	37.6
6-29		37.5
6-30		40.1
6-31	1000	36.1
6-32		35.7
6-39	1100	44.6
6-40		46.9
6-41		48.6
6-42	1200	31.6
6-44		29.6
6-48		29.7

Table C-3. EWC strength of LID-processed Ti-15-3 honeycomb core sandwich specimens

Specimen No.	Temp. (°F)	EWC strength (ksi)
15-25 15-26 15-27	Room Temp.	79.2 84.7 86.6
15-28 15-29 15-30	1000	47.6 46.3 46.2
15-37 15-38	1200	34.2 35.4
15-44 15-46	1300	31.0 31.1
15-47 15-48	1500	25.4 24.1

Table C-4. EWC strength of Pro-4-processed Ti-14-21 honeycomb core sandwich specimens

Specimen No.	Temp. (°F)	EWC strength (ksi)
AL-1 AL-2 AL-3	Room Temp.	62.8 60.0 63.5
AL-4 AL-5 AL-6	1000	41.5 39.4 39.0
AL-7 AL-8 AL-9	1200	34.9 32.1 36.8
AL-13 AL-14 AL-15	1300	31.1 31.9 32.5
AL-16 AL-20 AL-21	1500	21.3 19.6 22.0

REPORT DOCUMENTATION PAGE

Form Approved
OMB No. 07704-0188

1. AGENCY USE ONLY *(Leave blank)*	2. REPORT DATE	3. REPORT TYPE AND DATES COVERED
	June 1998	Technical Publication

4. TITLE AND SUBTITLE
Evaluation of the Transient Liquid Phase (TLP) Bonding Process for Ti_3Al-Based Honeycomb Core Sandwich Structure

5. FUNDING NUMBERS
522-12-11-01

6. AUTHOR(S)
R. Keith Bird
Eric K. Hoffman

7. PERFORMING ORGANIZATION NAME(S) AND ADDRESS(ES)
NASA Langley Research Center
Hampton, VA 23681-2199

8. PERFORMING ORGANIZATION REPORT NUMBER
L-17717

9. SPONSORING/MONITORING AGENCY NAME(S) AND ADDRESS(ES)
National Aeronautics and Space Administration
Washington, DC 20546-0001

10. SPONSORING/MONITORING AGENCY REPORT NUMBER
NASA/TP-1998-208421

11. SUPPLEMENTARY NOTES

12a. DISTRIBUTION/AVAILABILITY STATEMENT
Unclassified–Unlimited
Subject Category 26 Distribution: Standard
Availability: NASA CASI (301) 621-0390

12b. DISTRIBUTION CODE

13. ABSTRACT ***(Maximum 200 words)***

The suitability of using transient liquid phase (TLP) bonding to fabricate honeycomb core sandwich panels with Ti-14Al-21Nb (wt%) titanium aluminide (Ti_3Al) face sheets for high-temperature hypersonic vehicle applications was evaluated. Three titanium alloy honeycomb cores and one Ti_3Al alloy honeycomb core were investigated. Edgewise compression (EWC) and flatwise tension (FWT) tests on honeycomb core sandwich specimens and tensile tests of the face sheet material were conducted at temperatures ranging from room temperature to 1500°F.

EWC tests indicated that the honeycomb cores and diffusion bonded joints were able to stabilize the face sheets up to and beyond the face sheet compressive yield strength for all temperatures investigated. The specimens with the Ti_3Al honeycomb core produced the highest FWT strengths at temperatures above 1000°F. Tensile tests indicated that TLP processing conditions resulted in decreases in ductility of the Ti-14Al-21Nb face sheets.

Microstructural examination showed that the side of the face sheets to which the filler metals had been applied was transformed from equiaxed α_2 grains to coarse plates of α_2 with intergranular β. Fractographic examination of the tensile specimens showed that this transformed region was dominated by brittle fracture.

14. SUBJECT TERMS	15. NUMBER OF PAGES
Transient liquid phase; TLP; Mechanical properties; Titanium; Titanium-aluminide; Honeycomb core; Joining	46
	16. PRICE CODE: A03

17. SECURITY CLASSIFICATION OF REPORT	18. SECURITY CLASSIFICATION OF THIS PAGE	19. SECURITY CLASSIFICATION OF ABSTRACT	20. LIMITATION OF ABSTRACT
Unclassified	Unclassified	Unclassified	